AFGL-TR-86-0171(I)

SGI-R-86-126

ESTIMATING EXPLOSION AND TECTONIC RELEASE SOURCE PARAMETERS OF UNDERGROUND NUCLEAR EXPLOSIONS FROM RAYLEIGH AND LOVE WAVE OBSERVATIONS.

J.W. GIVEN
G.R. MELLMAN

SIERRA GEOPHYSICS, INC.
11255 KIRKLAND WAY
KIRKLAND, WASHINGTON 98033

JULY, 1986

FINAL REPORT - PART I
JANUARY 1985 - JANUARY 1986

AIR FORCE GEOPHYSICS LABORATORY
AIR FORCE SYSTEMS COMMAND
UNITED STATES AIR FORCE
HANSCOM AIR FORCE BASE, MASSACHUSETTS 01731

REPORT DOCUMENTATION PAGE

1a. REPORT SECURITY CLASSIFICATION UNCLASSIFIED	1b. RESTRICTIVE MARKINGS
2a. SECURITY CLASSIFICATION AUTHORITY	3. DISTRIBUTION/AVAILABILITY OF REPORT Distribution limited to US Government agencies and their contractors; Critical Technology; December 1986. Other requests for this document shall be referred to AFGL/LWH,Hanscom AFB,MA
2b. DECLASSIFICATION/DOWNGRADING SCHEDULE	
4. PERFORMING ORGANIZATION REPORT NUMBER(S) SGI-R-86-126	5. MONITORING ORGANIZATION REPORT NUMBER(S) 01731 AFGL-TR-86-0171(I)
6a. NAME OF PERFORMING ORGANIZATION SIERRA GEOPHYSICS, INC.	6b. OFFICE SYMBOL (If applicable) 4R088
6c. ADDRESS (City, State and ZIP Code) 11255 KIRKLAND WAY, SUITE 300 KIRKLAND, WA 98033	7a. NAME OF MONITORING ORGANIZATION AIR FORCE GEOPHYSICS LAB (AFSC) 7b. ADDRESS (City, State and ZIP Code) HANSCOM AFB, MA 01731
8a. NAME OF FUNDING/SPONSORING ORGANIZATION DEFENSE ADVANCED RESEARCH PROJECTS AGENCY	8b. OFFICE SYMBOL (If applicable) DARPA 9. PROCUREMENT INSTRUMENT IDENTIFICATION NUMBER F19628-85-C-0028
8c. ADDRESS (City, State and ZIP Code) 1400 WILSON BLVD. ARLINGTON, VA 22209	10. SOURCE OF FUNDING NOS.

PROGRAM ELEMENT NO.	PROJECT NO.	TASK NO.	WORK UNIT NO.
62714E	5A10	DA	AR

11. TITLE (Include Security Classification) SEE SECTION 16	
12. PERSONAL AUTHOR(S) J.W. GIVEN AND G.R. MELLMAN	
13a. TYPE OF REPORT FINAL-PART I	13b. TIME COVERED FROM JAN '85 TO JAN'86
14. DATE OF REPORT (Yr., Mo., Day) 1986 JULY	15. PAGE COUNT 79
16. SUPPLEMENTARY NOTATION ESTIMATING EXPLOSION AND TECTONIC RELEASE SOURCE PARAMETERS OF UNDERGROUND NUCLEAR EXPLOSIONS FROM RAYLEIGH AND LOVE WAVE OBSERVATIONS (U)	

17. COSATI CODES		
FIELD	GROUP	SUB. GR.

18. SUBJECT TERMS (Continue on reverse if necessary and identify by block number)
EXPLOSION
YIELD ESTIMATION
SURFACE WAVES
TECTONIC RELEASE

19. ABSTRACT (Continue on reverse if necessary and identify by block number)

The long-period (~20s) Rayleigh and Love waves for 37 events at Shagan River and 47 events at NTS are inverted for source parameters using the best available information on propagation for each source-receiver path and on excitation for each source region. At these periods, a three parameter source model is sufficient to describe the Rayleigh and Love wave amplitude and phase radiation patterns. However, the scatter in the source amplitudes dominates the radiation patterns of the surface waves, and additional station correction factors are necessary. These corrections are derived by simultaneously inverting many events from each test site for both the source parameters and station corrections. The inclusion of both Love and Rayleigh waves for events with a wide range of relative Love to Rayleigh wave excitation reduces possible bias in the station

20. DISTRIBUTION/AVAILABILITY OF ABSTRACT UNCLASSIFIED/UNLIMITED ☒ SAME AS RPT. ☐ ... USERS ☐	21. ABSTRACT SECURITY CLASSIFICATION UNCLASSIFIED
22a. NAME OF RESPONSIBLE INDIVIDUAL JAMES LEWKOWICZ	22b. TELEPHONE NUMBER (Include Area Code) 22c. OFFICE SYMBOL AFGL/LWH

corrections. This feature is important because no events at either test site are free from tectonic release effects.

The three source parameters do not constrain the size of the explosion source and further interpretation is necessary. In this study, m_b is assumed to reflect the explosion size. For an assumed tectonic release mechanism, we assume that there should be no correlation between (0.9 log M_I - m_b) and the amount of tectonic release present. At Shagan River, the tectonic release mechanism must include a substantial thrust-faulting component; at NTS, a strike slip fault model for the tectonic release is appropriate.

With the thrust fault model, the Rayleigh waves from the typical (median) event ($F = M_I/M_{DC} = 0.33$) at Shagan River are reduced in amplitude by the effects of tectonic release by 0.3 as measured by M_S (or log M_I). The overall correlation between log M_I and m_b at Shagan River is not expected to be any better than M_S and m_b. At NTS, log M_I, derived assuming tectonic release, is very similar to log M_I derived assuming no tectonic release. We do not anticipate any difference in the overall precision of yield estimates using log M_I or M_S at NTS. The explosion moments of the largest events at Shagan River are slightly higher ($\delta \log M_I = 0.1$) than the largest events analyzed from NTS. m_b at Pahute Mesa is 0.2 higher than an event at Yucca Flats with a similar M_I. For a given M_I, an event at Shagan River is expected to have an m_b that is 0.32 higher than an event at NTS.

TABLE OF CONTENTS

LIST OF FIGURES

LIST OF FIGURES
(continued)

LIST OF FIGURES
(continued)

LIST OF FIGURES
(Continued)

LIST OF TABLES

I. INTRODUCTION

The amplitudes of the long-period seismic waves, such as the 20 s Rayleigh waves (M_S), are often considered to be the most reliable data for estimating the yields of underground nuclear explosions at test sites where additional calibration information is not available. However, yield determination to better than 35% accuracy requires careful analysis to remove the large uncertainties in amplitudes caused by regional variations in surface-wave excitation and propagation. The largest source of error is due to differences in attenuation and elastic structure along the source to receiver paths, which often causes variations in amplitude among stations, as measured by M_S, of as much as 0.5. Theoretical calculations of the excitation of surface waves in typical geologic structures for test sites in the United States and the Soviet Union predict variations of 0.1 to 0.3 in M_S. In addition, the nuclear-explosion source is almost always accompanied by a nonexplosive source coincident in location and time with the explosion. The nonexplosive source is thought to be caused by the release of tectonic strain near the explosion, and thus, the amplitude effects depend on the orientation of the local stresses, which can be expected to differ considerably between test sites. The size of the tectonic release has not been observed to follow any predictable, (or even explicable) pattern in relation to other event parameters such as location, depth, or size.

The following is an analysis of the long period (17-60s) Rayleigh and Love waves from 47 events at NTS and 37 events at Shagan River. We outline a simple method for extracting source parameters, and we estimate the observable long-period source parameters from events in these regions. The source amplitudes were measured by applying the path corrections provided by J.L. Stevens, (personal communication) which were determined by techniques described in Stevens et al., (1982) and Bache et al. (1978). These path corrections are the result of a careful analysis of each source to receiver path and are based on realistic wave propagation models. Stevens (1986) made a careful study of the amplitudes of most of the events discussed in this report, although without correcting for the effects of tectonic release.

A simple, shallow source model is assumed; the tectonic release is assumed to be a double couple at a depth of 1 km. The source excitation is calculated using the best available information on the source structure for each region. Unfortunately, this source model does not allow us to determine uniquely the explosion size, and we must make other assumptions in order to interpret the size of the explosion and tectonic release. We will constrain the tectonic-release source orientation at each test site based on relative amplitude measurements using m_b and previous results from the literature obtained by other authors. These long-period source measurements can then be compared with other measures of explosion strength, e.g. yield, or m_b, to assess the reliability of surface-wave amplitude measurements as a means of yield estimation and to calibrate the Soviet test site at Shagan River.

II. LONG-PERIOD SOURCE MODEL FOR UNDERGROUND NUCLEAR EXPLOSIONS

The nonexplosive contribution to the seismic waves generated by the nuclear-explosion source was first observed by Oliver, 1960 and has since been intensively explored for events at the Nevada Test Site in the US (e.g. Toksoz et al., 1965; Aki et al., 1969; Aki and Tsai, 1972; Toksoz and Kehrer, 1972; Wallace et al., 1983, 1985; among many others), at the Shagan River region of eastern Kazakh in the Soviet Union (e.g. Rygg, 1976; North and Fitch, 1982; Helle and Rygg, 1985), and at the Soviet test site at Novaya Zemlya (Burger et al., 1985). There is a broad consensus among seismologists that the source of the nonexplosive seismic wave radiation is the release of tectonic strain, (termed tectonic release and hereafter referred as such) although the phenomena is not well understood. One mechanism, proposed by Press and Archambeau, (1968) and elaborated upon in Archambeau, (1972) is that the stress release occurs in the fractured zone surrounding the nuclear explosion. Another mechanism, argued for by Aki et al., (1969) and Aki and Tsai, (1972) is that the release of stress occurs by triggered motion on nearby faults. This interpretation has been corroborated by many observations of faulting and aftershocks coincident with and following nuclear tests at NTS (Bucknam, 1969; Hamilton and Healy, 1969). Wallace et al., 1983 further argues for triggered fault motion although their model differs significantly from the Aki and Tsai (1972) models and may more appropriately be called "driven" fault motion. All of these mechanisms can be described by combining double couples with an explosion source and are virtually indistinguishable at the periods of interest for surface waves (~20 s). The details of the spectra at shorter periods (1-10s) await further investigation. The several mechanisms have very different effects on the spectra of the shorter-period seismic waves, which are sensitive to the time functions of the sources and the spatial and temporal relations between the nuclear explosion and the tectonic release sources.

At periods of greater than 15 s, the explosive and nonexplosive sources can be considered to be coincident in space and time. Some indication of a tim. delay in the tectonic component can be found in analysis of events with large amounts of tectonic release at the Shagan River test site by Rygg (1976) and Goforth et al. (1982). Events with large components of tectonic release often show apparent time delays of several seconds. However these time delays only introduce a small phase change at the long periods of interest (>15 s) and the amplitude effects are ignored.

The source of the underground nuclear explosion is assumed to be adequately modeled at long periods by a shallow, (depth ~ 1 km) point moment tensor source with a step function time history. In the following we adopt a cartesian coordinate system at the source with x north, y east, and z down. The azimuth, ϕ, will be defined as clockwise from north. The Rayleigh wave source radiation pattern as a function of frequency, ω, and source depth, z_s, can be written as

$$V_R(\omega,\phi) = P_R^1(\omega,z_s)[-M_{xy}\sin 2\phi - 1/2\,(M_{xx} - M_{yy})\cos 2\phi] +$$

$$S_R^1(\omega,z_s)[M_{zz} - 1/2\,(M_{xx} + M_{yy})] + N_R^1(\omega,z_s)[M_{xx} + M_{yy} + M_{zz}]/3 -$$

$$iQ_R^1(\omega,z_s)[M_{xz}\cos\phi + M_{yz}\sin\phi\,] \qquad (1)$$

where P_R^1, S_R^1, Q_R^1, and N_R^1 are excitation functions as described in Kanamori and Stewart, (1976) and Kanamori and Given (1980). P_R^1, S_R^1, and Q_R^1 are the excitation functions for a vertical strike-slip fault, a 45 dip-slip fault, and a vertical dip slip fault; N_R^1 is the excitation function for an explosion. The tectonic release is assumed to be due to deviatoric sources, so that the isotropic moment, M_I, given by $1/3(M_{xx} + M_{yy} + M_{zz})$, is assumed to be a measure of the explosion size. Similarly, the excitation function for the Love waves can be written

$$V_L(\omega,\phi) = P_L^1(\omega,z_s)[\ -M_{xy}\cos 2\phi + 1/2(M_{xx} - M_{yy})\sin 2\phi] +$$

$$iQ_L^1(\omega,z_s)\ [M_{xz}\sin\phi - M_{yz}\cos\phi] \qquad (2)$$

Equations 1 and 2 can be simplified by recognizing that the contributions from the moment tensor elements, M_{xz} and M_{yz}, are negligible at these periods for very shallow sources. Further simplification can be obtained by using some relations among the excitation functions,

$$P_R^1 = 1/3\ S_R^1 - 1/3\ N_R^1 \qquad (3)$$

If we define

$$S_0 = 1/2\ (M_{xx} + M_{yy}) - (1/3)\ [(S_R^1 + N_R^1)/P_R^1]\ M_{zz}$$

$$S_1 = 1/2\ (M_{xx} - M_{yy}) \qquad (4)$$

$$S_2 = M_{xy}$$

then Equations 1 and 2 can be rewritten

$$V_R = P_R^1\ (S_0 + S_1\cos 2\phi + S_2\sin 2\phi) \qquad (5)$$

$$V_L = P_L^1\ (S_1\sin 2\phi - S_2\cos 2\phi) \qquad (6)$$

One further shallow source approximation is useful,

$$1/3\ (S_R^1 + N_R^1) \sim P_R^1\ (\alpha^2 - 2\beta^2)/\alpha^2 \qquad (7)$$

which gives

$$S_0 \sim 1/2\ (M_{xx} + M_{yy}) - [(\alpha^2 - 2\beta^2)/\alpha^2]\ M_{zz} \qquad (8)$$

Figures 1 and 2 illustrate the applicability of the different approximations. The approximation given in Equation 7 is not very good at periods below 40 s at NTS, however the effect on the determination of explosion moments is small since M_I is the average of M_{xx}, M_{yy}, and M_{zz}. Equation 5 is similar to expressions derived by Toksoz and Kehrer, 1972 and North and Fitch (1981) to analyze surface waves from underground nuclear explosions. S_0, S_1, and S_2 cannot uniquely constrain the isotropic moment without further assumptions about the non-explosive source mechanism. We will assume that the tectonic release occurs by slip along faults in the vicinity of the shot point. Therefore the source is a combined double couple and explosion. We will further need to constrain the orientation of the double-couple; this can be accomplished by observing how log M_I varies with m_b for different amounts of tectonic release. A useful parameter, introduced by Toksoz et al. (1965) to characterize the amount of tectonic release is F which we define here as

$$F = M_{DC}/M_I \qquad (9)$$

where M_{DC} is the double couple moment. (This definition is different than many of those previously introduced that have an additional factor of about 3/2 to indicate the difference in excitation between a strike-slip double-couple source and an explosion.) At Shagan River, events with large amounts of Love wave radiation have Rayleigh waves that are reversed in polarity relative to events with small Love wave amplitudes suggesting that tectonic release is caused by thrust faulting. This mechanism implies that, for events with moderate tectonic release ($\sim F<0.5$) overall Rayleigh-wave amplitudes decrease with increasing tectonic release. On the other hand, the average Rayleigh wave

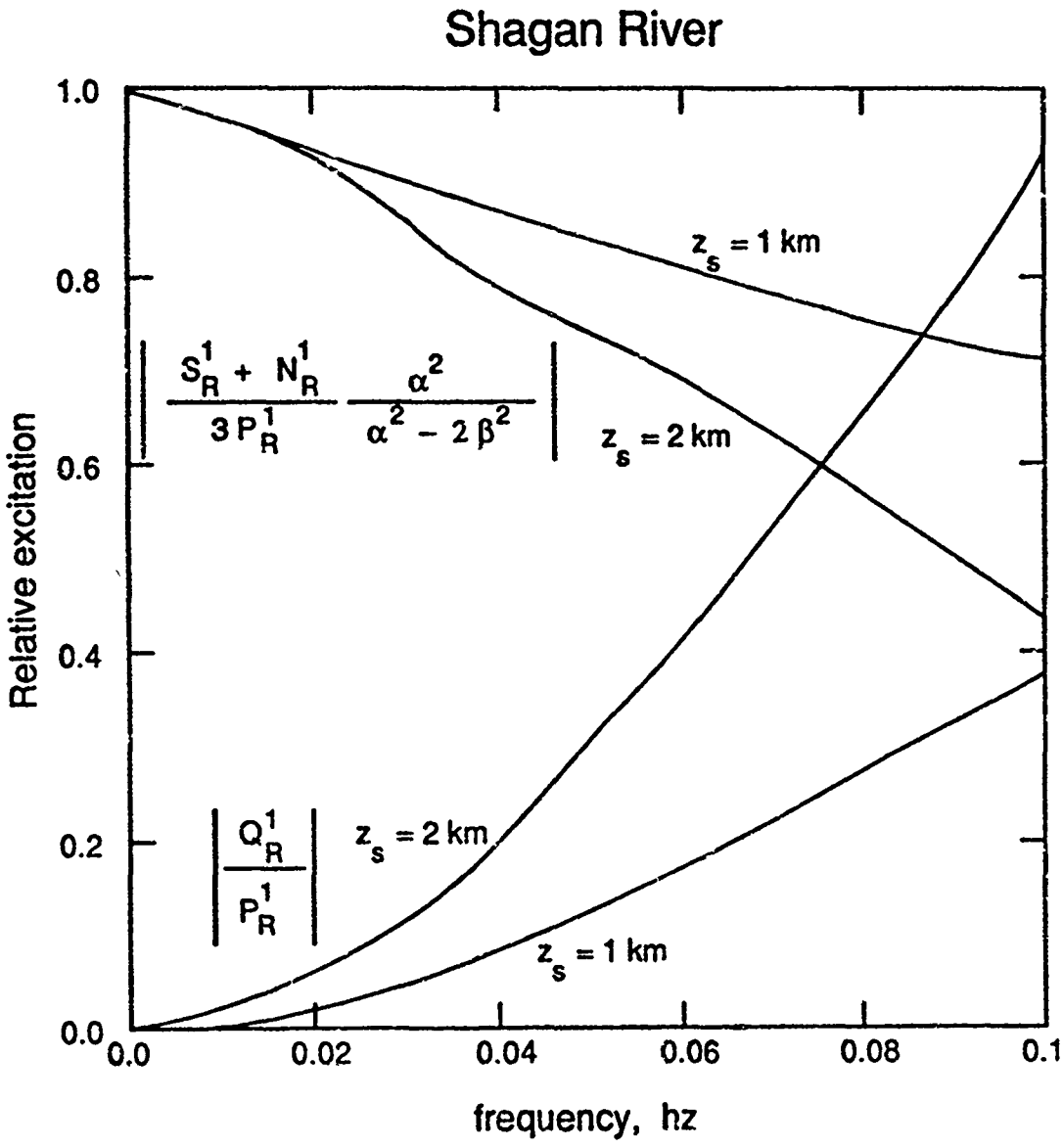

FIGURE 1. The amplitude of the excitation functions for M_{zz}, M_{xz}, and M_{yz} relative to P_R^1 for events located at Shagan River. For the purposes of subsequent inversion, Q_R^1 is considered negligible and $1/3 (S_R^1 + P_R^1) (\alpha^2/\alpha^2 - 2\beta^2) = P_R^1$.

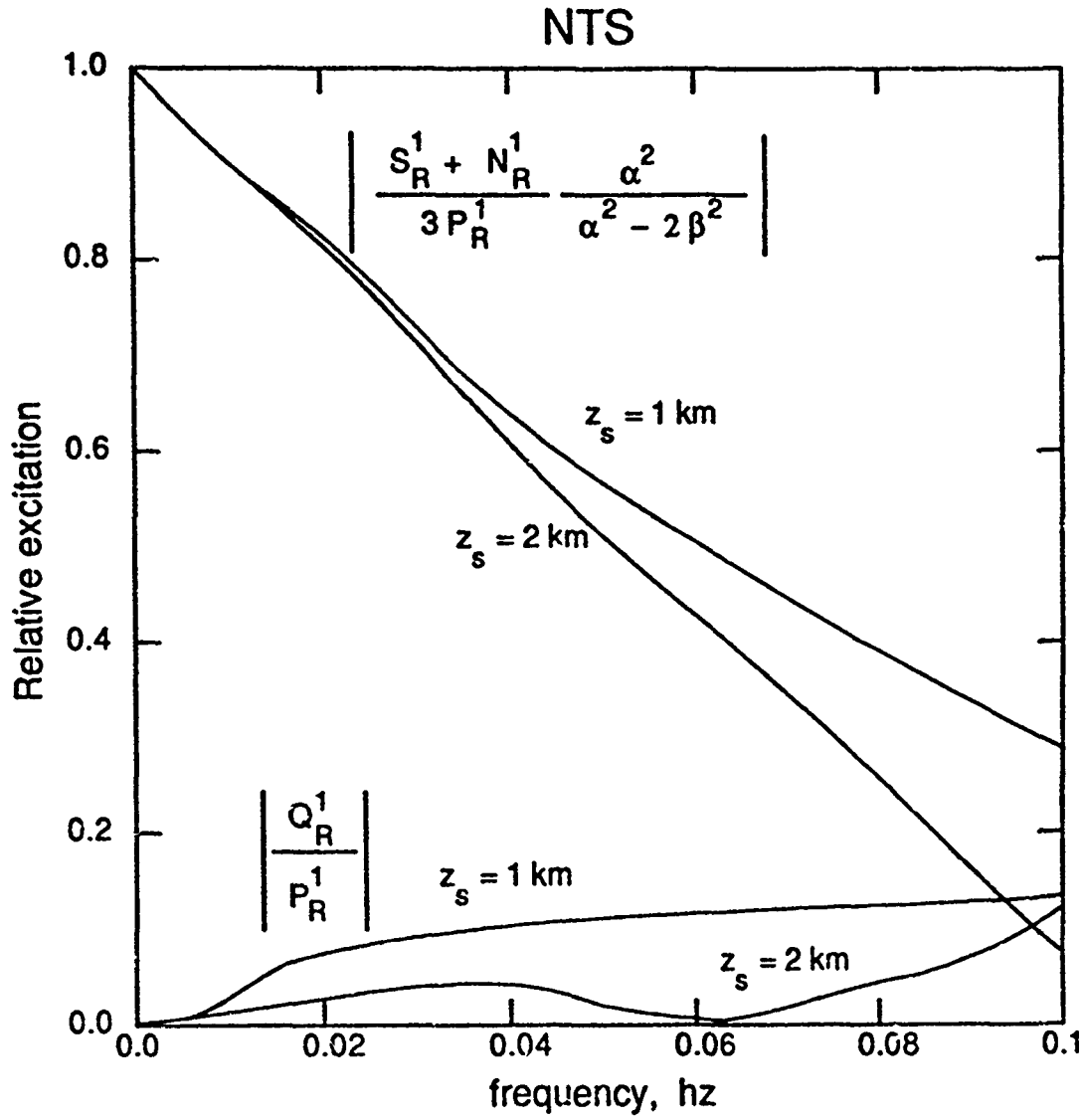

FIGURE 2. The amplitude of the excitation functions for M_{zz}, M_{xz}, and M_{yz} relative to P_R^1 for events located at NTS.

amplitudes at NTS do not change noticeably with increasing tectonic release suggesting that a mechanism near strike slip is more appropriate, as discussed in Wallace et al. (1983, 1985).

We will constrain the double couple contribution to the source by specifying the dip and slip of the fault and using S_1 and S_2 to determine the strike. If we define

$$S_1' = [(S_1)^2 + (S_2)^2]^{1/2} \tag{10}$$

then

$$M_{DC} = S_1'/[(\sin^2 \lambda \sin^2 2\delta)/4 + \cos 2\lambda \sin^2 \delta] \tag{11}$$

$$M_I = - (P_R^1/N_R^1)\, S_0 - (S_R^1/2P_R^1)\, M_{DC} \sin \lambda \sin 2\delta \tag{12}$$

or, using Equation 7,

$$M_I = (\alpha^2/2\beta^2)\, S_0 + [(3\alpha^2/4\beta^2) - 1]\, M_{DC} \sin \lambda \sin 2\delta \tag{13}$$

The strike of the fault, ϕ_f, is given by the solution to the equations

$$\sin 2\phi_f = [M_{DC}/ (S_1')^2]\, (\cos \lambda \sin \delta\, S_1 - 1/2 \sin \lambda \sin 2\delta\, S_2)$$

$$\cos 2\phi_f = [M_{DC}/ (S_1')^2]\, (-1/2 \sin \lambda \sin 2\delta\, S_1 - \cos \lambda \sin \delta\, S_2) \tag{14}$$

The source region structure is the same as that used by Stevens (1986) modified from a surface wave analysis of the NTS to Tucson, Arizona path (Bache et al., 1978) to be consistent with the upper-mantle structure of Anderson and Hart (1976; 1978) and with the Pahute Mesa shallow structure determined by Bache et al. (1975). The Shagan River structure is modified from the surface wave analysis of the

Shagan River to the SRO station MAIO (Mashad, Iran) path. The upper 1.5 km of the Shagan River structure is assigned an (α,β, and ρ) of (5 km/s, 2.7km/s, and 2.7 g/cm3) to be compatible with weathered hard rock values.

The calculation of M_l, using Equation 13, depends on the elastic structure ($\alpha^2/2\beta^2$) in the immediate source vicinity, while the source parameter S_0 depends on the excitation function, P_R^1, which is a continuous function of depth and is therefore relatively insensitive to small scale velocity variations. For the source structure at NTS, ($\alpha^2/2\beta^2$) should be 2.7 while at Shagan River this ratio is 3.4. There is little constraint on the local Poisson ratio at either test site yet the difference implied by these two structures would increase M_l at Shagan River by 0.09 relative to NTS. We have chosen to make the shot point velocity ratio the same for both test sites and use ($\alpha^2/2\beta^2$) of 1.71.

III. DATA ANALYSIS

With observations of the source spectra, Equations 5 and 6 can be inverted by a least squares method for the observable source parameters. The source spectra are obtained from a deconvolution of the observed Rayleigh and Love wave spectra, U_R and U_L,

$$U_R(\omega) = V_R(\omega)\, T_R(\omega) \exp(\gamma_R(\omega) r) \exp(i\omega r/C_R(\omega) - i\pi/4)(\sin\Delta)^{1/2} I(\omega) \quad (15)$$

$$U_L(\omega) = V_L(\omega)\, T_L(\omega) \exp(\gamma_L(\omega) r) \exp(i\omega r/C_L(\omega) + i\pi/4)(\sin\Delta)^{1/2} I(\omega) \quad (16)$$

where $I(\omega)$ is the instrument response, r is epicentral distance in km, Δ, the epicentral distance in degrees, γ is the attenuation factor, $C(\omega)$ is the phase velocity, and $T(\omega)$ is a transmission coefficient to account for differences in source and receiver structure.

In the period range of 15 - 60 s, γ and C are very dependent on the source to receiver paths. To invert Equations 5 and 6 it is necessary to have accurate estimates of γ and C for each path. Stevens et al., 1982 and Stevens, 1985 calibrate the propagation paths from the Shagan River test site to the SRO and ASRO stations, and from NTS to SRO, ASRO, WWSSN and CSN (Canadian Seismograph Network) stations. They measured Rayleigh-wave phase velocity for each path assuming that the initial phase is known. These measurements were inverted for the effective plane-layered elastic structure between the source and each receiver. Finally, using estimates of the source structure and the source depth, the Rayleigh-wave amplitude spectra are inverted for the source moment and attenuation structure. Gross earth attenuation models were used to constrain the deep attenuation structure for each path to reduce the strong tradeoffs that occur between estimated source moments and attenuation. The absence of any dependence of the source moments, derived by individual station analysis, on epicentral distance provides an additional check on the attenuation models. The moments

determined by such an inversion procedure may be contaminated by non-isotropic source effects. However if the tectonic release is adequately explained by the models discussed in the previous section, then the shape of the amplitude and phase spectra are unaffected by the tectonic release. Thus the method of determining the attenuation and phase velocity, described by Stevens et al. (1982), is insensitive to the amount of nonisotropic radiation, even if the derived source moment does not represent the true explosion size.

Significant signal to noise enhancement is achieved by removing propagation and instrument phase from the observed Rayleigh wave spectra and recomputing the time-domain waveform, which is an application of the phase-matched filter method described by Herrin and Goforth (1977). The surface wave train will then be compressed into a pulse while the noise, in general, will remain dispersed. The observed surface wave pulse can then be rewindowed using a much smaller time window that excludes much of the noise in the original window, before deconvolution of the remaining amplitude effects.

The Rayleigh observations for the Shagan River events are from 14 SRO/ASRO stations distributed around the test site as shown in Figure 3. We excluded the Love-wave observations from ANMO, BCAO, ZOBO and CHTO because of poor signal quality. From NTS we used WWSSN, CSN (Canadian Seismograph Network) and SRO/ASRO stations. Figures 4 and 5 show the distribution of stations around NTS. The data were restricted to those travel paths for which path corrections were available (Stevens, personal communication). For several events at NTS, we improved the station average by using additional stations for which detailed path corrections had not been specifically derived. For these stations, there were nearby source-receiver path corrections available. If the assumptions behind the derivation of the path corrections were accurate, these stations can be used to estimate source amplitudes (although not necessarily phase) reasonably well.

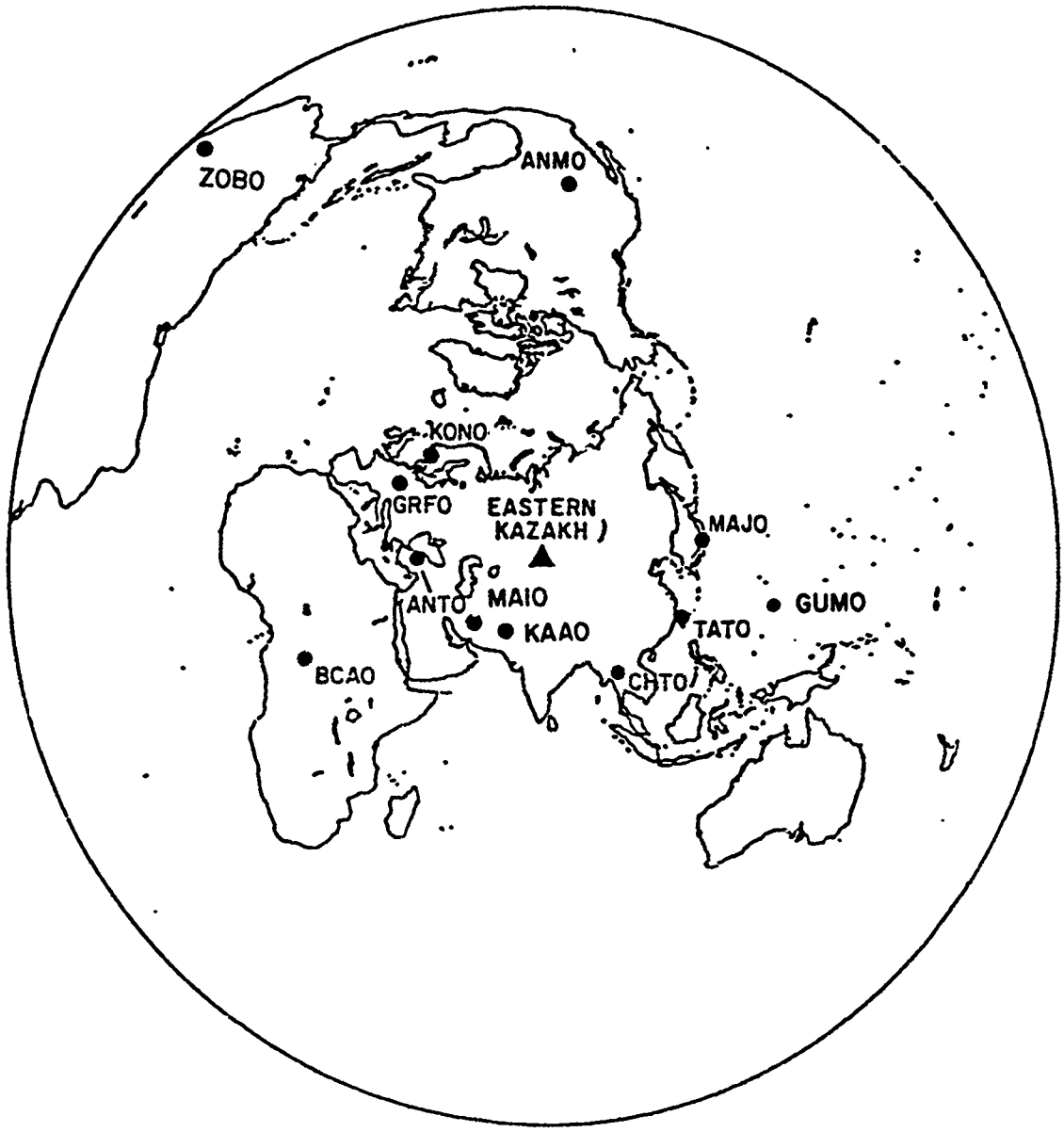

FIGURE 3. Azimuthal, equidistant map showing location of SRO/ASRO stations around Shagan River.

FIGURE 4. Azimuthal equidistant map showing location of SRO/ASRO station around NTS.

FIGURE 5. Azimuthal equidistant map showing location of WWSSN/CSN stations around NTS.

Figures 6 and 7 show the results of applying the phased matched filters to the Rayleigh-wave seismograms from the Shagan River events recorded at stations KONO and MAJO. Most of the seismograms are similar, however significant phase distortion is evident for some events. Some events are reversed in polarity at some statons, as previously observed by Rygg (1976) and North and Fitch (1981). Station MAJO (Figure 7) is one of those that shows polarity reversals frequently; KONO shows a reversal only when the entire network is reversed. The Rayleigh waves from these completely reversed events are highly contaminated by tectonic release and exhibit large Love-wave amplitudes.

The Love waves are processed using phase-velocity and attenuation estimates calculated from the plane-layered models that were derived from the inversion of the Rayleigh-wave data. Earth models derived solely from Rayleigh wave data are frequently not good enough to predict Love-wave propagation properties. When the estimated phase velocities were used as phase-matched filters for the Love-wave seismograms, significant time compression was often obtained, but the initial phase estimates were not reliable.

Figures 8 and 9 show the results of applying the phase-matched filter to the Love waves at GRFO and MAJO. There is more variability in the signal quality of the Love waves than seen in the Rayleigh waves as a result of variation in the strength of the Love wave radiation relative to the explosion generated Rayleigh waves, and as a result of slight rotations to the mechanism of the tectonic release. A new observation, seen in Figure 8, is the nearly complete polarity reversal for some events observed at GRFO. Although a large shift in tectonic release mechanism is not necessary to explain a shift in the Love wave polarities, these two events apparently have very different tectonic release orientation as seen in the next section.

The observed consistency of the Love-wave phase from event to event provided a way to accurately use the Love wave amplitudes and phase in evaluating the tectonic release. First, a preliminary examination of

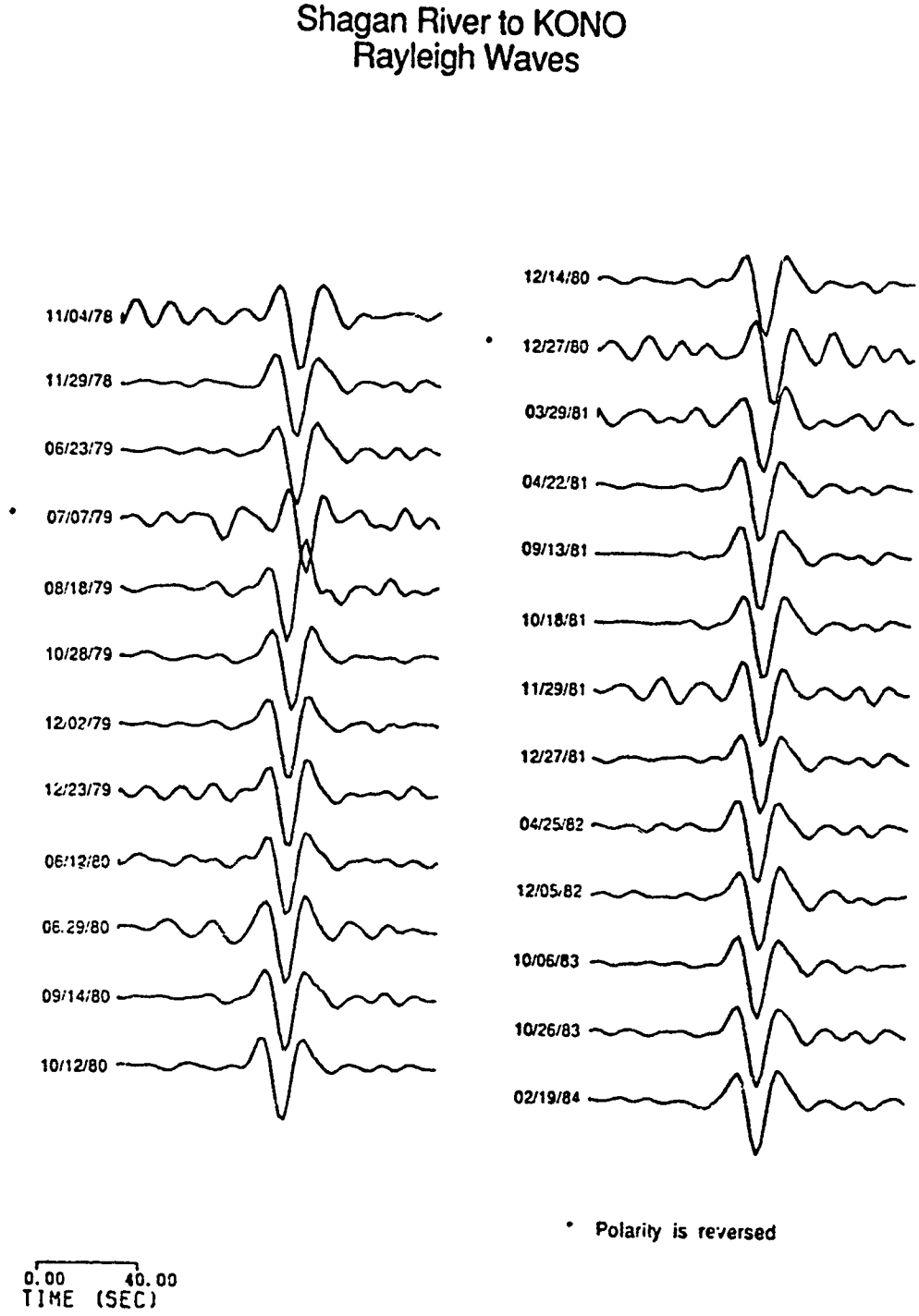

FIGURE 6. Rayleigh wave observations of Shagan River events at station KONO after application of phase matched filter.

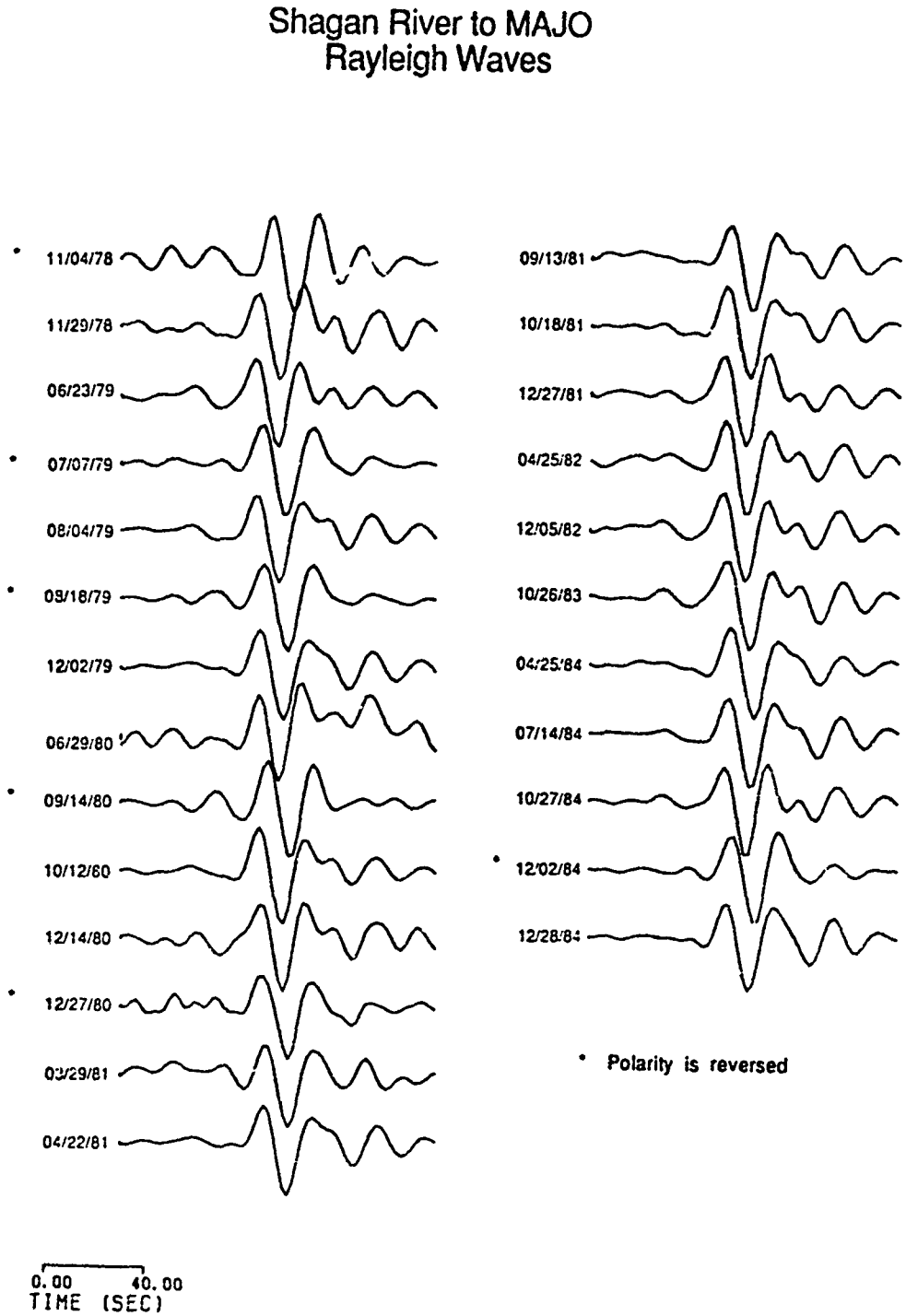

FIGURE 7. Rayleigh wave observations of Shagan River events at station MAJO after application of phase matched filter.

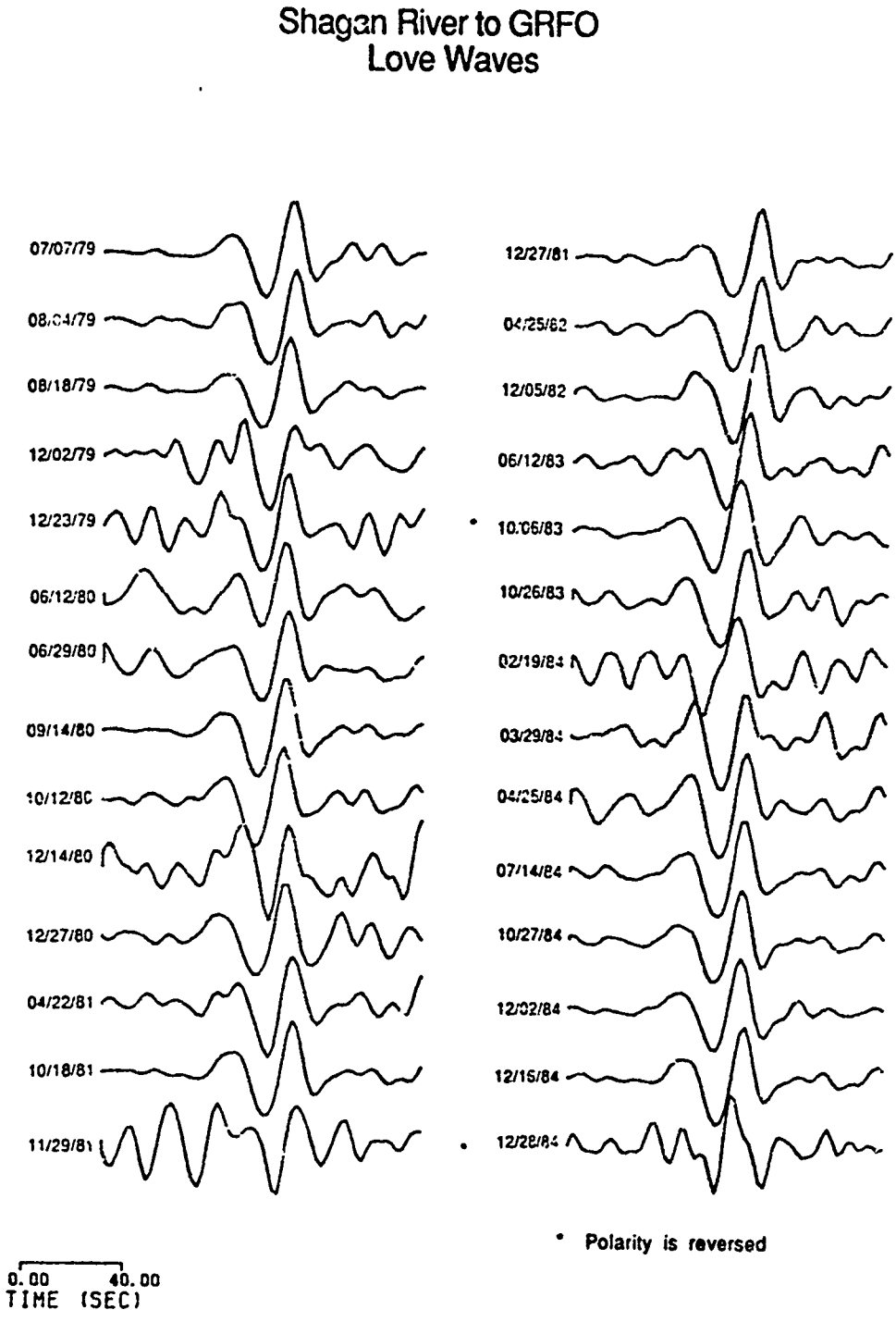

FIGURE 8. Love wave observation of Shagan River events at station GRFO after application of phase-matched filter.

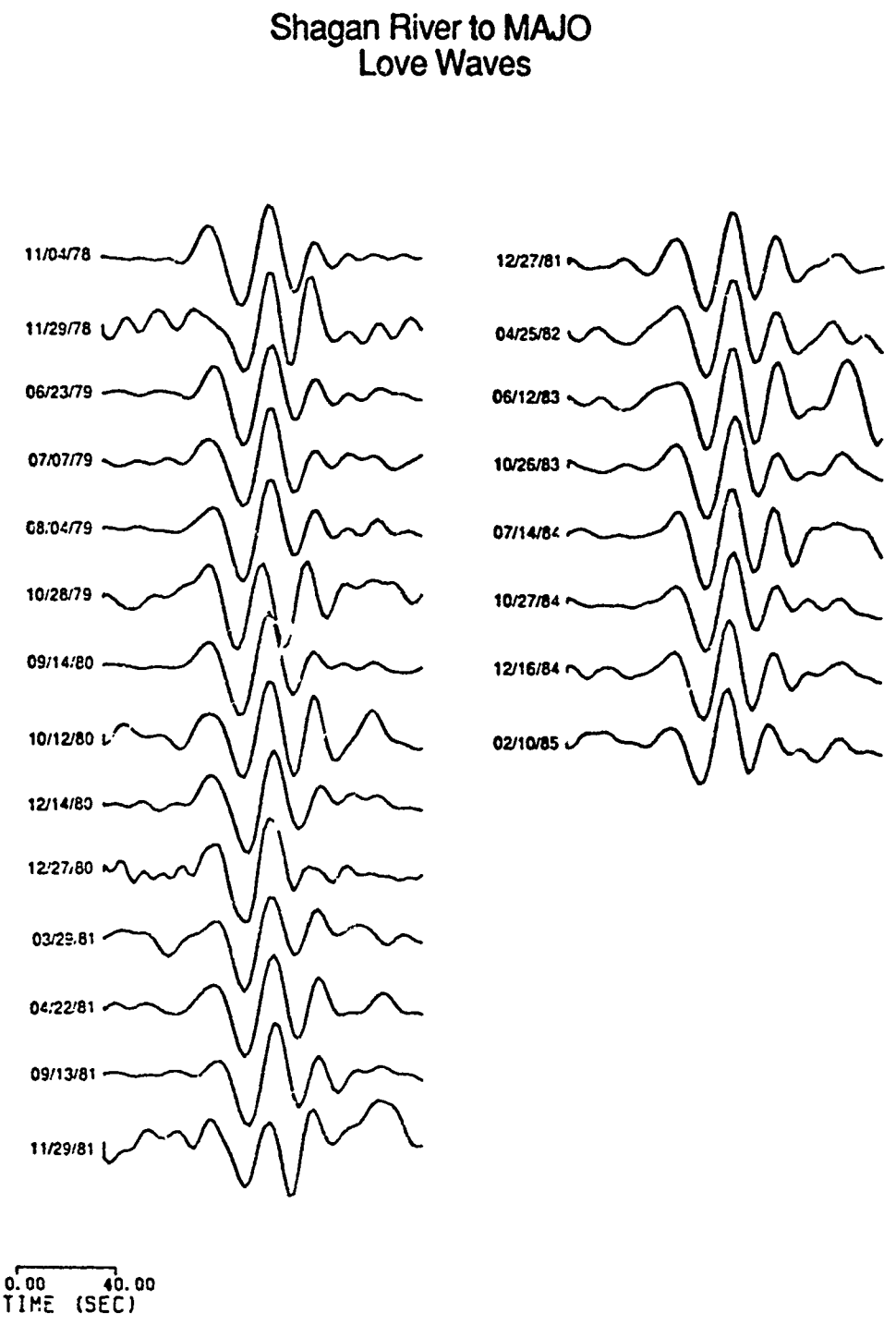

FIGURE 9. Love wave observations of Shagan River events at station MAJO after application of phase-matched filter.

the Rayleigh waves revealed the predominate orientation of the tectonic release. Using this orientation, we can assign a "normal" initial phase to each Love wave receiver. The occasional reversed phase Love wave observation can be included by simply using the opposite polarity for that station and event.

Variations of a magnitude unit or more between individual stations are not uncommon in body and surface wave amplitude studies and station corrections are usually necessary to handle these variations, particularly when network coverage varies substantially from event to event. Despite the careful analysis applied to the surface wave excitation and propagation from these events, stations with similar azimuths still show amplitude variations of almost a factor of 2. Love wave amplitude variations are even larger since the propagation has not been carefully calibrated and since the Love waves are particularly sensitive to lateral heterogeniety. These amplitude variations completely dominate the radiation pattern caused by the tectonic release, and additional station amplitude corrections are necessary to remove these effects. For simplicity, these corrections will be frequency independent multipliers to the observed amplitudes.

The correction factors are determined by simultaneously inverting a number of events for both mechanism and station correction. Combining Equations 5 and 6,

$$V_i^j = \exp_{10}^{(a_i)} \; G_{ik}^j \; S_{ik}^j \qquad (17)$$

where V_i^j is the observed spectral displacement, averaged over the frequency band of interest, for the j-th event at the i-th station. The Rayleigh and Love wave observations are treated as independent. G_{ik}^i are the excitation functions and S_k^i are the observabie parameters for each event. Equation 17 is nonlinear and is inverted using a linearized least-squares method. An initial guess to the observable parameters is obtained using station correction factors, a_i of 0. In subsequent steps,

the station corrections and revised source parameters are obtained until no further improvement can be made. At each step, the solution for the station corrections was damped to stabilize the inversion.

It was decided that, since the Rayleigh wave path corrections have been carefully analyzed, the Rayleigh wave amplitude correction factors (the a_i's in Equation 17 above) should have a zero mean. This is a subjective requirement. Some of the propagation paths cross several tectonic provinces and the plane-layered models may not be expected to accurately predict the amplitudes of the observed surface waves. These stations may be less reliable and it is difficult to determine how to assess the reliability in a quantitative way. Requiring the Rayleigh wave corrections to average zero may demand that the Love-wave corrections have a non-zero mean since the source excitation and amplitude corrections are not necessarily consistent. For instance at Shagan River, the Love-wave corrections average about 0.1, indicating that the attenuation models are not compatible, or that the source structure does not give the correct relative Love to Rayleigh wave excitation.

Table 1 gives the correction factors for Shagan River. NTS was subdivided into Pahute Mesa and Yucca Flats when it was observed that significant waveform differences occur between the two sites for some stations. Table 2 gives the corrections for these two sites. Most station corrections do not differ markedly between Pahute Mesa and Yucca Flats, however OTT, OGD and WES show significant differences that we attribute to unexplained near-source effects on the excitation.

The resulting corrections enhance the amount of tectonic release that accompanies the explosion over that which would be determined if no corrections were used. For example stations KONO, CHTO and SHIO, which are in the directions of the maximum amplitudes of the Rayleigh wave radiation pattern, have positive corrections, while KAAO and MAJO are negative. In addition, the Love wave corrections are on the average about 0.08. Although this bias is not necessarily apparent when the entire network is considered, these five stations are

TABLE 1

SHAGAN RIVER STATION CORRECTIONS

	RAYLEIGH	LOVE
ANMO	-0.05	
ANTO	-0.01	
BCAO	-0.04	
CHTO	0.29	
GRFO	0.17	0.11
GUMO	-0.20	-0.15
KAAO	-0.11	0.18
KONO	0.15	0.31
MAIO	0.04	0.06
MAIO	-0.21	-0.01
SHIO	0.15	0.18
TATO	0.36	0.11
ZOBO	0.15	

TABLE 2

NTS STATION CORRECTIONS

	YUCCA		PAHUTE	
	R	Love	R	Love
AAM	-0.09	-0.13	-0.01	-0.09
ALQ	0.08	-0.04	0.05	-0.02
BLA	-0.01	0.01	-0.11	0.00
BLC	0.10		-0.06	
COL	0.00	0.24	-0.04	0.12
COR	0.16		0.12	
DAL	0.03		0.17	
EDM	-0.20		-0.23	
FCC	-0.03		-0.07	
FFC	0.05		-0.02	
FLO	0.00			
FVM	0.12	0.18	-0.07	0.09
FSI	0.35		0.44	
GOL	-0.23	0.08	-0.15	0.09
JCT	-0.08	-0.17	-0.08	-0.08
LHC	-0.04		-0.12	
LON	0.19	-0.04	0.21	-0.13
LUB	0.14	0.07	0.03	-0.08
MBC	-0.26		-0.28	
MSO	0.04	-0.09	0.01	-0.22
OGD	-0.01	0.03	0.01	-0.06
OTT	-0.2		0.07	
OXF	0.12		0.19	
PHC	-0.35		-0.46	
PNT	0.19		0.16	
RES	-0.03		-0.03	
SCP	-0.18	-0.05	-0.06	-0.06
SES	0.18		0.23	
SHA	0.05	0.18	0.06	-0.13
VIC	0.06		0.05	
WES	-0.10	-0.05	-0.06	0.00

TABLE 2
(continued)

NTS STATION CORRECTIONS

	YUCCA		PAHUTE	
	R	Love	R	Love
ANTO	.007			
BCAO	-0.18		-0.12	
BOCO	-0.05		-0.03	
CTAO	0.08		0.09	
GRFO	-0.06		0.09	
KONO	0.02		-0.03	
MAIO	-0.06		-0.10	
MAJO	0.26		0.25	
TATO	-0.09		-0.12	
ZOBO	0.22		0.29	

particularly important for determining the tectonic release for many of the events. Thus an event that appears isotropic using the Rayleigh wave amplitudes at these stations actually has significant tectonic release. It is important to consider how this bias arises in the inversion procedure.

That some of the apparent bias is probably due to real propagation effects can be seen by examining the events with the lowest tectonic release events. Figure 10 shows the station corrections plotted as a function of azimuth derived in three different ways. One way was to use those events with normal Rayleigh-wave phase and invert Equation 7 with the constraint that these events have no tectonic release. This is essentially the procedure used by Stevens (1986) and our results are slightly different only because of differences in the frequency bandwidths used in each analysis. Since this method includes events with significant amounts of tectonc release, an azimuthal bias is to be expected, if not necessarily observed. Another way to determine station corrections is to use those two events, 2 December 1979 and 10 February 1984, that exhibit very low tectonic release as exhibited by low amplitude Love-wave radiation. As seen in Figure 10 an azimuthal component to the stations corrections (note KAAO, MAJO, KONO, SHIO and CHTO) becomes necessary to make these two events appear isotropic. However, these events are not isotropic since some Love wave radiation is observed (no surface wave observations from Shagan River events are not contaminated by tectonic release) and hence we can conclude that an even larger azimuthal component to the Rayleigh-wave corrections may be necessary. Neither of these two methods makes use of the Love-wave amplitudes. Changes in the Love wave amplitudes are related to asymmetry in the Rayleigh-wave radiation pattern and can be used to remove any azimuthal bias that may be present in the initial path corrections.

The bias in the corrections is determined by the relative excitation of the Love and Rayleigh waves and the wide range of F-values and Love-wave amplitudes of the events used in determining the corrections. As a simple experiment, we assume that we can determine the maximum and minimum of the Rayleigh wave radiation patterns. Then,

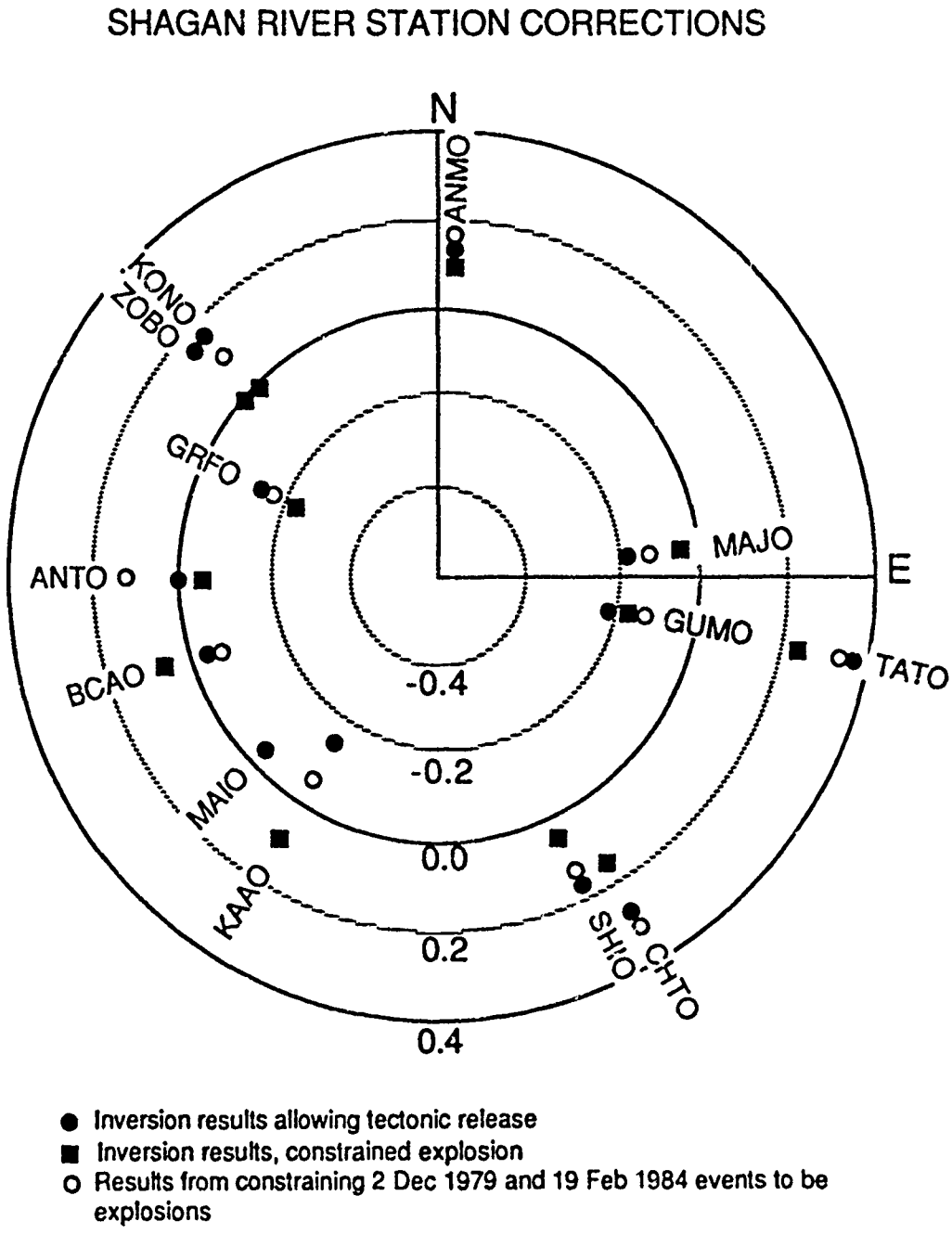

FIGURE 10. Azimuthal distribution of station corrections (a_i in Equation 17) for Shagan River events.

$$R_{max} = a_R P_R^1 (S_0 + S_1) \quad (18)$$

$$R_{min} = P_R^1 (S_0 + S_1)/a_R \quad (19)$$

where a_R describes the amplitude bias of the correction factors; ideally a_R would be one. Similarly, the Love waves give

$$L_{max} = a_L P_L^1 S_1' \quad (20)$$

These equations can be combined to yield

$$[R_{max} - (a_R)^2 R_{min}]/a_R = (P_R^1 P_L^1/a_L \quad (21)$$

Equation 21 shows how the Rayleigh and Love wave biases are related. Obviously, P_L^1, P_R^1, and a_L tradeoff directly. If only one estimate of L_{max} is available, then the excitation functions and both a_R and a_L will tradeoff. With several, well-determined estimates of L_{max}, corresponding to a wide range of S_1', a_R and $P_R^1 P_L^1/a_L$ can be constrained independently. Although we do not prove it here, the inversion technique using Equation 17 is analogous to the experiment described above. Although there is no reason to expect that the path corrections from Stevens, 1982 may have an azimuthal bias, we argue that our inversion method gives the best unbiased estimates of the amount of tectonic release, given the constraints that the a_i's must sum to zero and the prespecified source excitation.

The determination of the station corrections at NTS was inhibited by the poor quality of the limited Love-wave data. Only data for events subsequent to 1977 were available; fortunately, several of these events showed little Love wave excitation, and so reasonable estimates of the Rayleigh-wave station corrections were possible. The azimuthal distribution of the path corrections for Yucca Flats is shown in

Figure 11. There are systematic differences between the corrections derived assuming an explosion source and those corrections obtained allowing tectonic release but this is to be expected since there is significant tectonic release present for most of the events. Although the station corrections do not scatter randomly about zero independent of azimuth, there do not seem to be any adverse sin 2ϕ, cos 2ϕ patterns in the corrections that indicate a bias possibly related to the source mechanism.

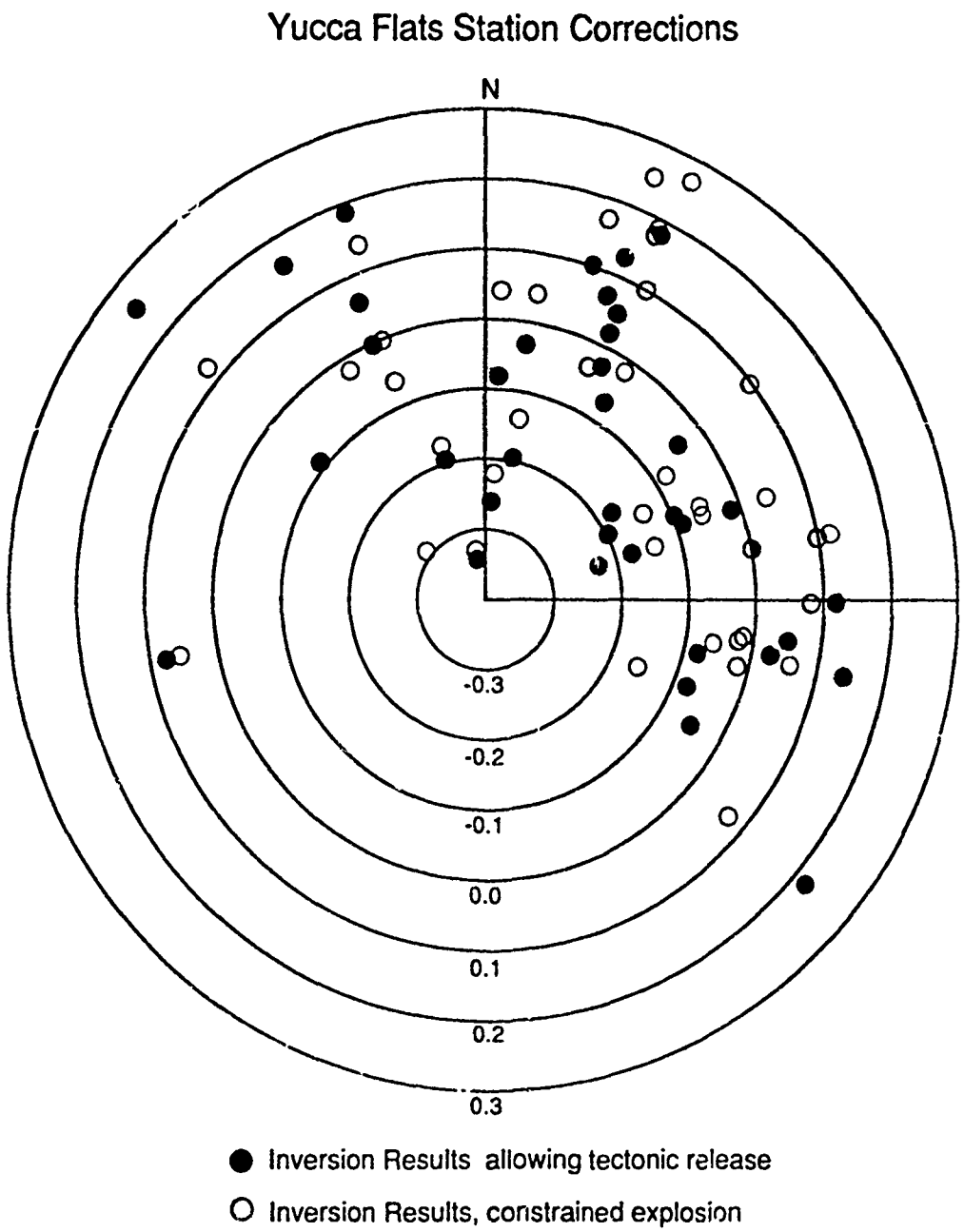

FIGURE 11. Azimuthal distribution of station corrections (a_i in Equation 17) for Yucca Flats events.

IV. RESULTS

A. SHAGAN RIVER RESULTS

The inversion results for the Shagan River events are given in Table 3. These results are presented assuming a thrust mechanism, which gives the maximum possible isotropic moment. Figures 12 through 15 show examples of the radiation patterns of several events with increasing amounts of tectonic release, relative to the explosion strength, at approximately the same orientation. In Figure 14, sufficient tectonic release is present to make the event appear as a strike slip earthquake with a four lobed Rayleigh wave radiation pattern, (although there is no difficulty distinguishing this event as an explosion). For events containing the highest tectonic release, a two lobed pattern re-emerges as seen in Figure 15. However, the maximum amplitude of the lobes is rotated 90^{0} relative to the low tectonic release events and the polarity is reversed at all azimuths.

Three Shagan River events showed Love-wave polarities that differed at several stations from the relative to the rest of the events. These events are shown in Figures 16 through 18 and have tectonic release orientations that significantly differ from the rest of the population. As can be guessed from the station coverage shown in the figures, the solutions of two of these cannot be considered very reliable. The results from 14 December 1980 are, however, well constrained, and represents a significant outlier from the normal population.

The mechanism of tectonic release is inferred by making a number of assumptions. First, the mechanism is assumed to be a double couple. Second, since two of the fault parameters must be constrained for each event, it is assumed that the slip and dip angles are the same for each event. Finally, m_b is assumed to reflect the isotropic part of the source. The validity of this last assumption has been studied in the literature by Bache and Lambert (1976), Wallace et al. (1985), Lay et al.(1984) and Burger et al. (1985) with varying results. There is little evidence at Shagan River for any body wave amplitude anomalies that

Table 3. Shagan River inversion results.

DATE	M_I	M_{DC}	F	STRIKE	log(M_I)	m_b
08/29/78	8.1	5.46	0.67	320.	15.91	5.95
09/15/78	11.3	3.25	0.29	327.	16.05	5.99
11/04/78	8.7	5.34	0.61	324.	15.94	5.56
11/29/78	12.1	4.04	0.33	333.	16.08	6.07
06/23/79	17.6	6.46	0.37	320.	16.25	6.22
07/07/79	7.5	11.20	1.49	321.	15.88†	5.83
08/04/79	18.7	6.22	0.33	321.	16.27	6.16
08/18/79	10.4	8.67	0.84	318.	16.02	6.12
10/28/79	19.6	7.22	0.37	339.	16.29	5.96
12/02/79	13.8	2.04	0.15	327.	16.14	6.01
12/23/79	8.0	2.32	0.29	322.	15.90	6.18
06/12/80	2.9	1.08	0.37	329.	15.46†	5.59
06/29/80	4.1	1.35	0.33	345.	15.61†	5.74
09/14/80	21.2	13.60	0.64	320.	16.33	6.21
10/12/80	15.4	4.49	0.29	333.	16.19	5.90
12/14/80	12.7	5.63	0.44	307.	16.10	5.95
12/27/80	2.8	4.54	1.62	322.	15.45†	5.88
03/29/81	5.4	3.33	0.61	332.	15.74	5.61
04/22/81	13.0	3.32	0.26	328.	16.11	6.05
09/13/81	18.1	6.37	0.35	316.	16.26	6.18
10/18/81	14.5	4.37	0.30	331.	16.16	6.11
11/29/81	7.1	1.73	0.24	333.	15.85†	5.73
12/27/81	15.4	4.87	0.32	336.	16.19	6.31
04/25/82	14.6	4.82	0.33	334.	16.17	6.1 *
12/05/82	15.6	5.19	0.33	328.	16.19	6.1
06/12/83	19.8	4.49	0.23	333.	16.30	6.1
10/06/83	18.4	4.12	0.22	252.	16.27†	6.0
10/26/83	21.3	8.56	0.40	318.	16.33	6.1
02/19/84	9.5	1.08	0.11	328.	15.98	5.8
03/29/84	10.9	3.43	0.31	314.	16.04†	5.9
04/25/84	15.3	2.96	0.19	341.	16.18†	5.9
07/14/84	19.2	4.94	0.26	333.	16.28	6.2
10/27/84	17.4	6.08	0.35	328.	16.24	6.2
12/02/84	12.7	8.77	0.69	333.	16.11†	5.8
12/16/84	22.7	6.65	0.29	334.	16.36	6.1
12/28/84	7.9	1.20	0.15	267.	15.90†	6.0
02/10/85	16.1	3.27	0.20	326.	16.21	5.9

Units of M_I and M_{DC} are 10^{15} N-m

m_b's are from Marshall, Bache, and Lilwall (1984)

* After 04/25/82 m_b's are from NEIS

† Indicates solutions with estimated errors > 0.06 in log M_I

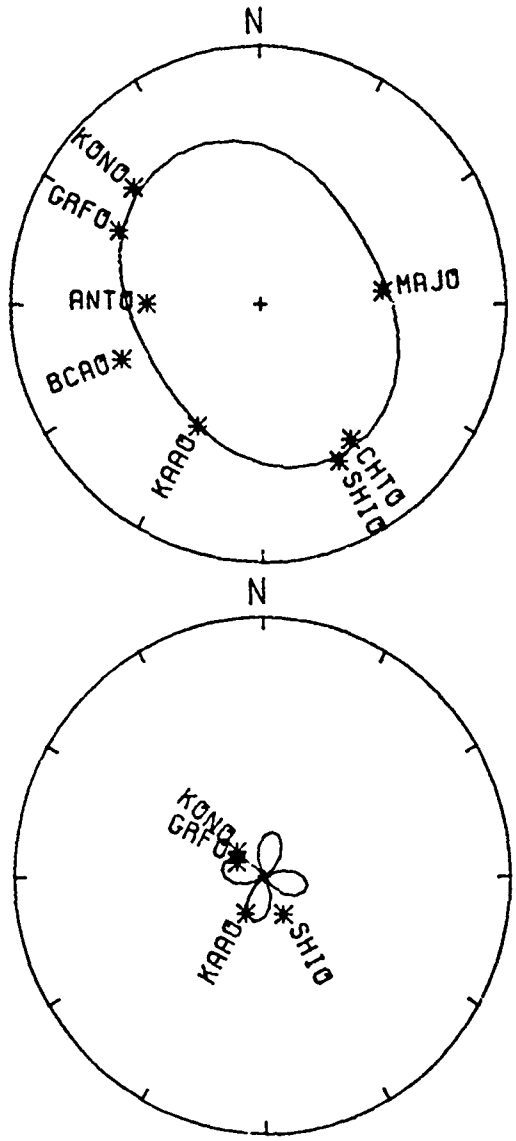

FIGURE 12. Observed and calculated amplitude radiation patterns for the Rayleigh waves (top) and Love waves (bottom) for the Shagan River event of 2 December 1979. The observed amplitudes include all path corrections and station corrections and an averaged over the period range from 17-45 s. The amplitude scales are linear with the value at the circle being the maximum amplitude indicated. The amplitude scale is the same for both plots.

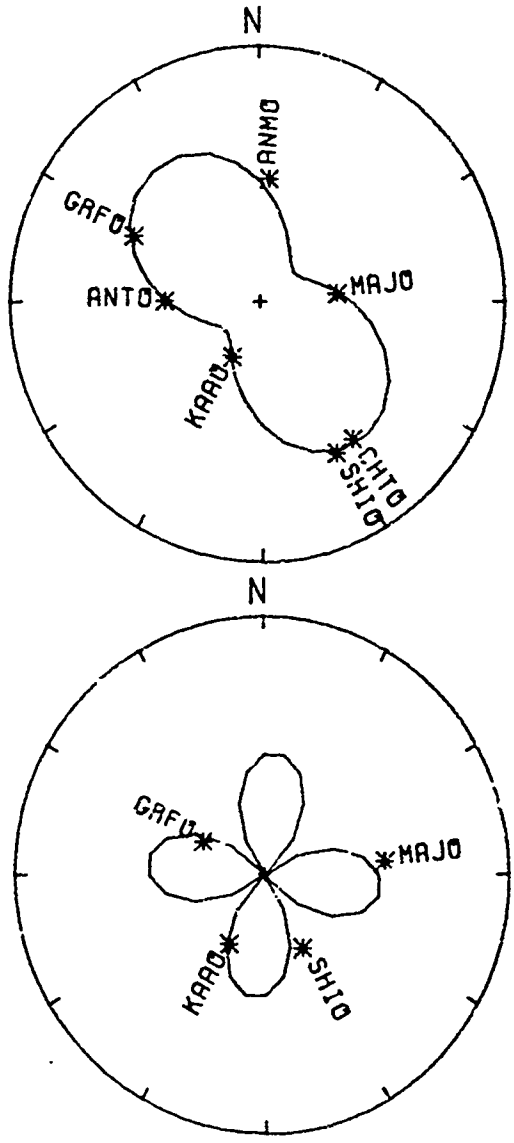

FIGURE 13. Observed and calculated amplitude radiation patterns for the Rayleigh waves (top) and Love waves (bottom) for the Shagan River event of 4 August 1979. See caption for Figure 12.

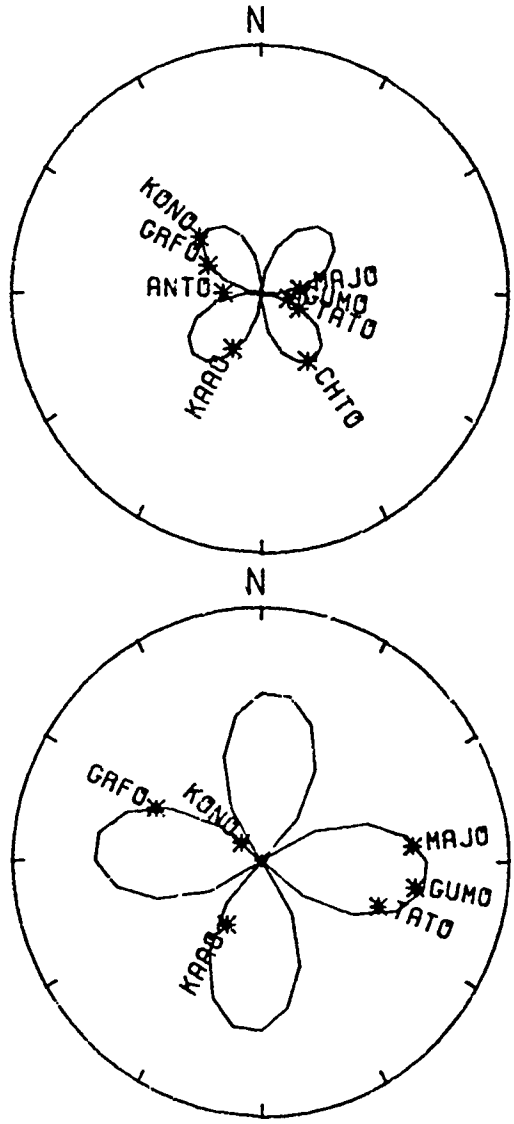

FIGURE 14. Observed and calculated amplitude radiation patterns for the Rayleigh waves (top) and Love waves (bottom) for the Shagan River event of 14 September 1980. See caption for Figure 12.

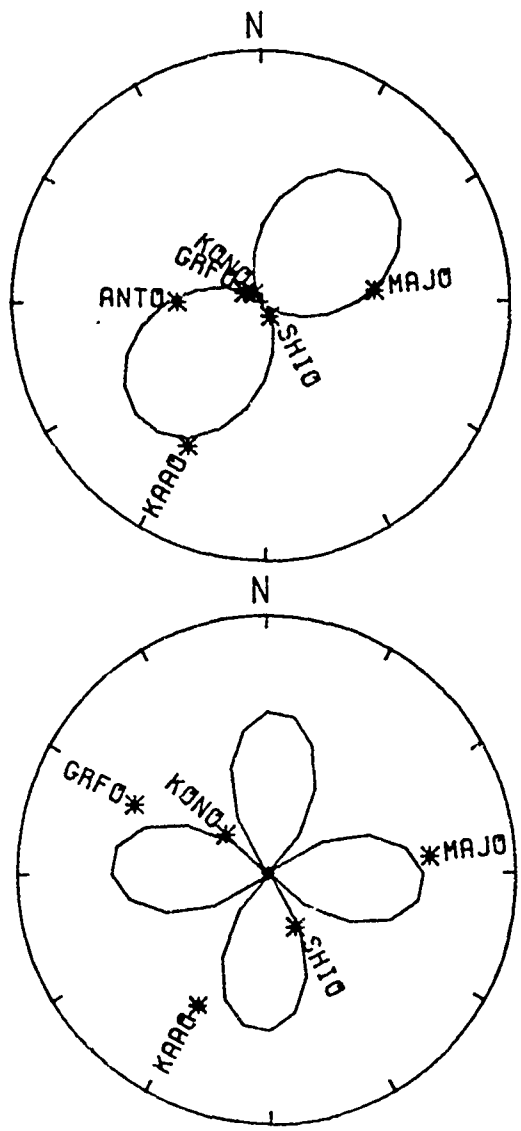

FIGURE 15. Observed and calculated amplitude radiation patterns for the Rayleigh waves (top) and Love waves (bottom) for the Shagan River event of 7 July 1979. See caption for Figure 12.

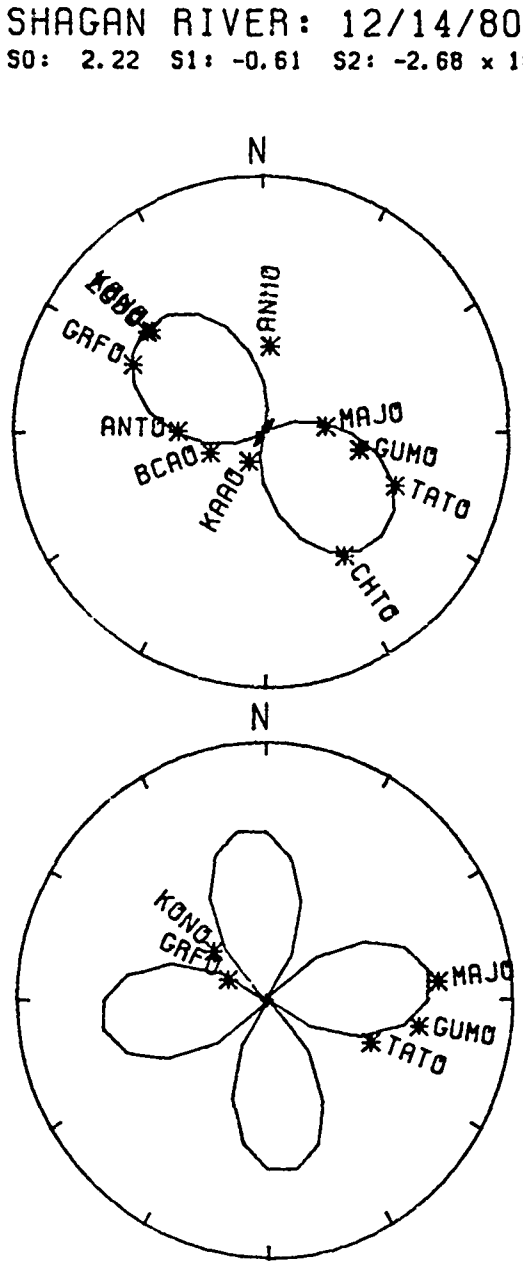

FIGURE 16. Observed and calculated amplitude radiation patterns for the Rayleigh waves (top) and Love waves (bottom) for the Shagan River event of 14 December 1980. See caption for Figure 12.

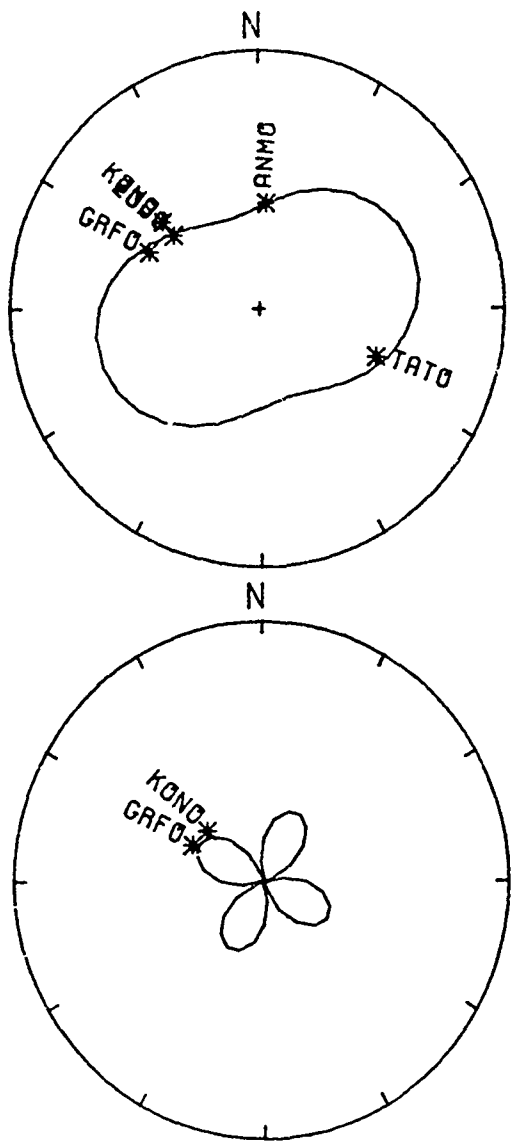

FIGURE 17. Observed and calculated amplitude radiation patterns for the Rayleigh waves (top) and Love waves (bottom) for the Shagan River event of 6 October 1983. See caption for Figure 12.

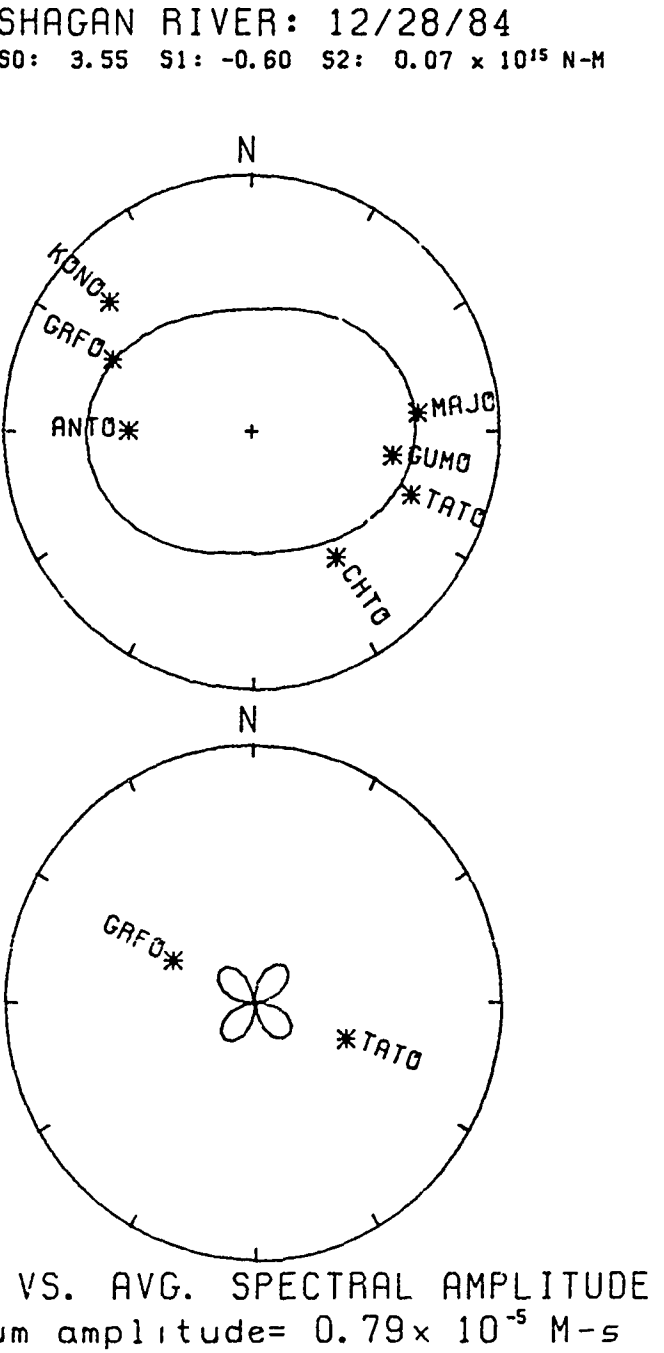

FIGURE 18. Observed and calculated amplitude radiation patterns for the Rayleigh waves (top) and Love waves (bottom) for the Shagan River event of 28 December 1984. See caption for Figure 12.

correlate with tectonic release. However, thrust faulting would introduce only subtle changes in the azimuthal radiation pattern and in the teleseismic waveforms, while possibly increasing the overall amplitudes significantly. This would lead us to overestimate the isotropic moments from m_b.

We assume m_b scales according to

$$m_b = 0.9 \log M_I + d \qquad (22)$$

since the data here cannot constrain the scaling. The value, d, for each event should, therefore, be independent of the amount of tectonic release present if the correct mechanism is used to obtain M_I. Using m_b's from a study by Marshall et al., 1984, Figure 19 shows (0.9 log M_I - m_b), plotted against the F_{TH} for two fault orientations, thrust faulting (dip 45^o, slip 90^o) and oblique-slip faulting (45, 45). The oblique slip mechanism lowers the estimated moments for the "average event" (F = 0.3) by about 0.1 unit. Using the oblique mechanism, the high F_{TH} events are typically low with respect to the rest of the population; some events appear to be implosions if this mechanism is proposed. Furthermore, the low F_{TH} events are higher than the rest under the oblique fault hypothesis. These observations slightly favor the thrust fault mechanism over the oblique faulting. The assumption of thrust faulting further provides the upper bound on M_I as can easily be seen using the results of Section 11.

A perhaps more convincing comparison of (0.9 log M_I - m_b) and the amount of tectonic release is apparent if we regionalize the events and restrict the analysis to those events that occur in the southwest part of the test site. Figure 20 shows a map of the events using locations from Marshall et al., 1984. Figure 21 shows the correlation between log M_I and m_b and the basis of the regionalization. Bache et al., 1985 have documented spectral and waveform differences between the southwest and northeast regions of Shagan River. Figure 22 shows only the

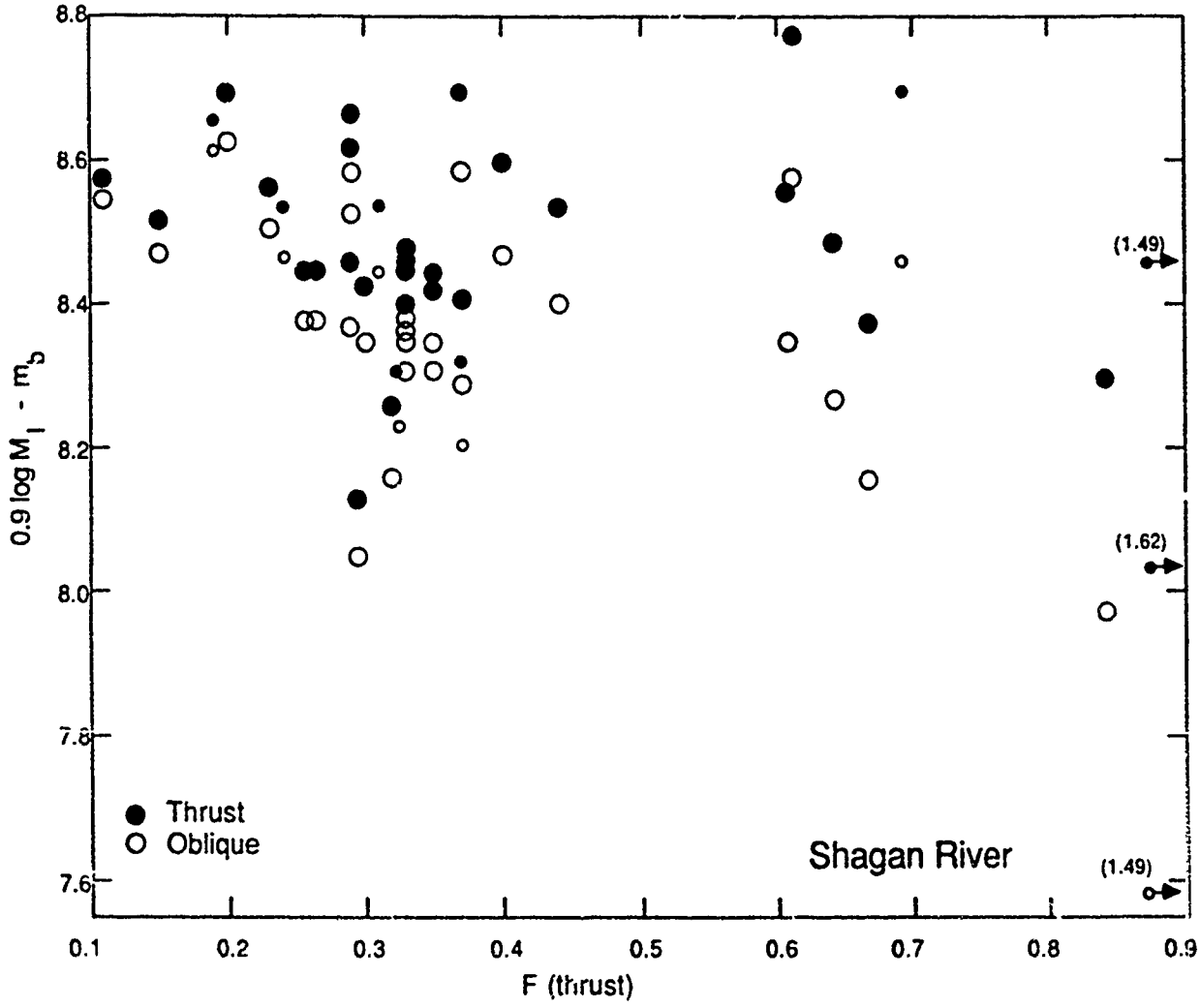

FIGURE 19. Variation of m_b - log M_l relation at Shagan River as a function of F' for two possible tectonic release mechanisms: thrust (dip = 45°, slip = 90°) and oblique (dip = 45°, slip = 45°). F is calculated assuming a thrust mechanism for both cases. If correct mechanism is chosen, and all events are similar, then there should be no apparent trend in the quantity 0.9 log M_l - m_b with F'.

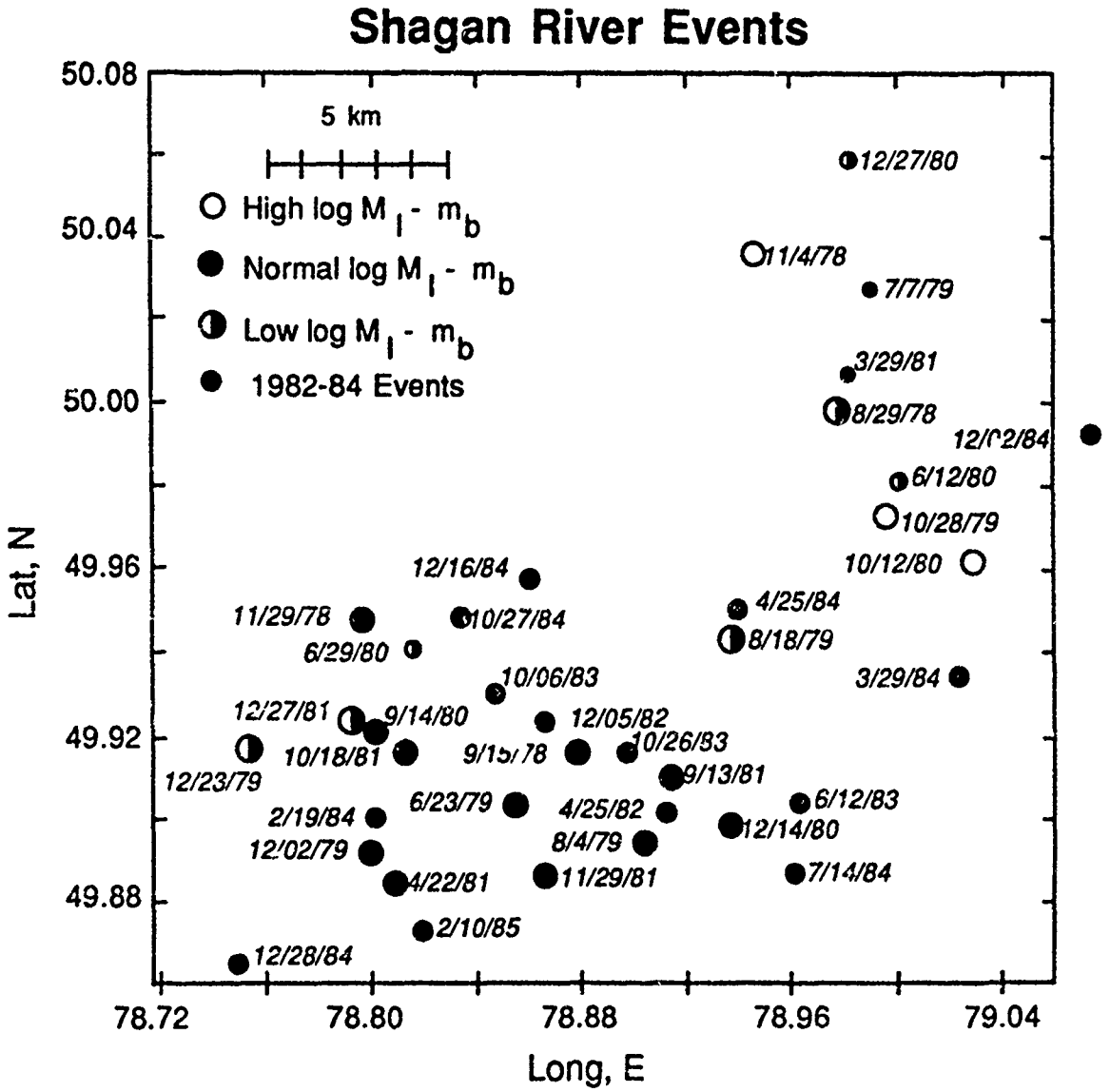

1978-82 Locations from Marshall, Bache, and Lilwall (1984)
1983-84 Locations from NEIS

FIGURE 20. Location of Shagan River events.

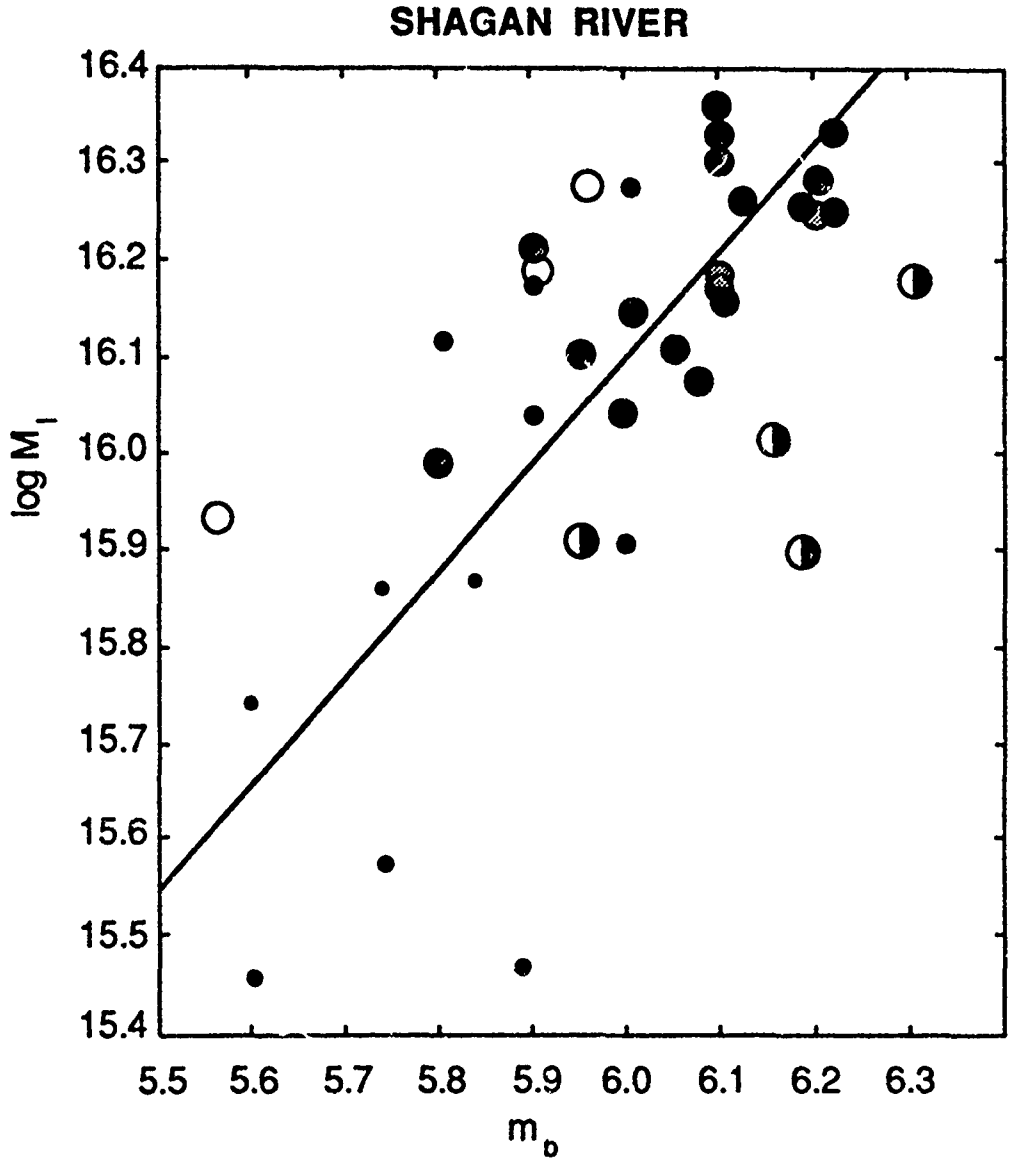

FIGURE 21. m_b vs. log M_l for Shagan River events. The line represents the best fit to all events and is given by the equation m_b - 0.9 log M_l - 8.48.

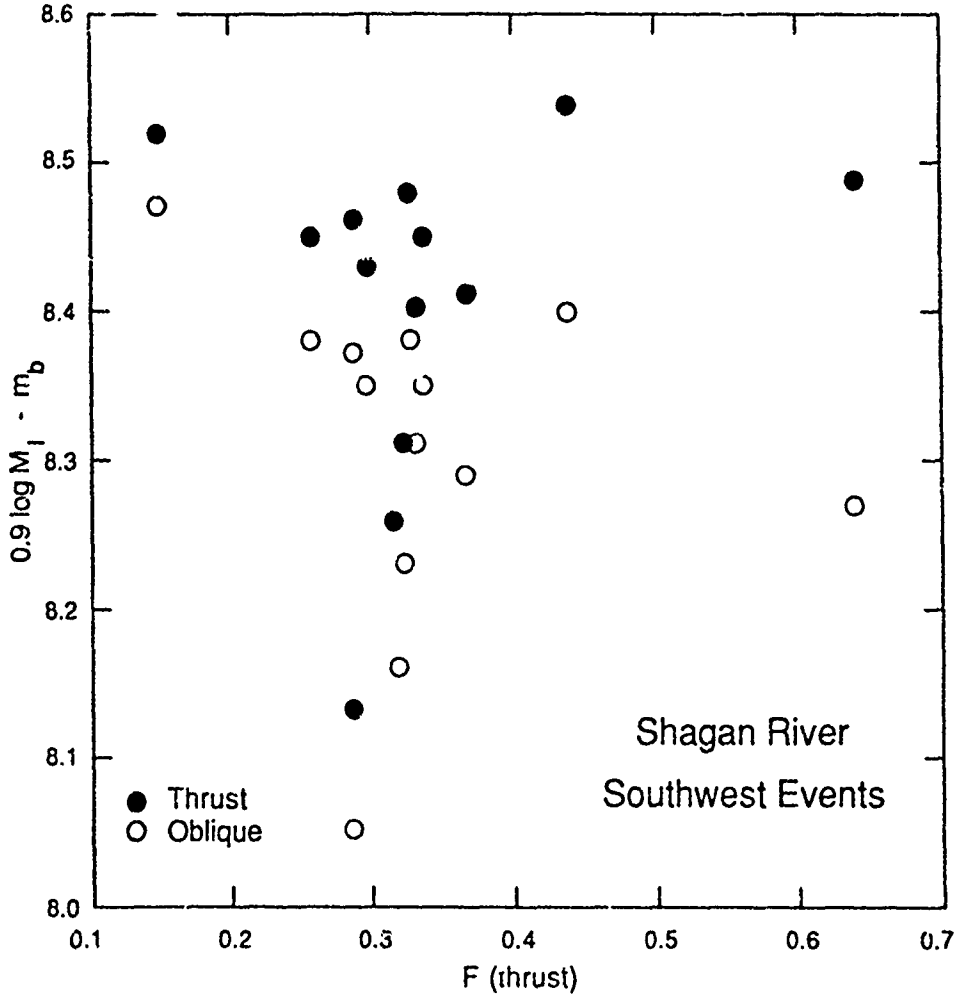

FIGURE 22. Variation of m_b - log M_l relation at Shagan River as a function of F for two possible tectonic release mechanisms for the southwestern Shagan River events prior to April 1982. See caption, Figure 23.

southwestern events for which consistent m_b measurements are available. There is now a more apparent trend with f for the oblique slip model that disappears when a thrust fault is assumed. If we disregard the recent events, for which only NEIS m_b's are available, then the events with high (0.9 log M_l - m_b) are exclusively in the northeast part of the test site, which may suggest that the material properties are significantly different, or that the tectonic release mechanism varies. That the tectonic release mechanism occasionally may change significantly at Shagan River is implied by the three events shown in Figures 16 - 18. The most extreme deviation is the event of 28 December 1984, apparently located far to the southwest and apparently with a radiation pattern that is rotated about 90^0 for the rest of the events.

The Shagan River observation can be interpreted with other, equally plausible assumptions. For instance, the fault plane (e.g., strike and dip) can be fixed and the slip angle on the fault allowed to vary. Another model would be to allow m_b to reflect both the isotropic part of the source and some part of the tectonic release component. At Shagan River, the predominate orientation of the tectonic release would tend to enhance the m_b. This model would require some currently unavailable method of estimating the time function of the tectonic release, but may explain some events with anomolously low M_l relative to m_b. The log M_l derived here by assuming thrust faulting estimates the maximum effect of tectonic release on the surface wave amplitudes under the assumption that the source mechanism of the tectonic release is a double couple. Because it is a maximum estimate, it is probabiy biased high, although as we have seen, some events clearly require thrust faulting to explain the source as an explosion combined with a double couple.

Several examples of the radiation pattern of NTS events are given in Figures 23 through 26. There is considerable variability in the data quality from these events that is evident in the scatter between observed data and the computed radiation patterns. While no event was unambiguously phase reversed, the initial phase estimates were not nearly as consistent as the Shagan River data. In addition the time

THIS
PAGE
IS
MISSING
IN
ORIGINAL
DOCUMENT

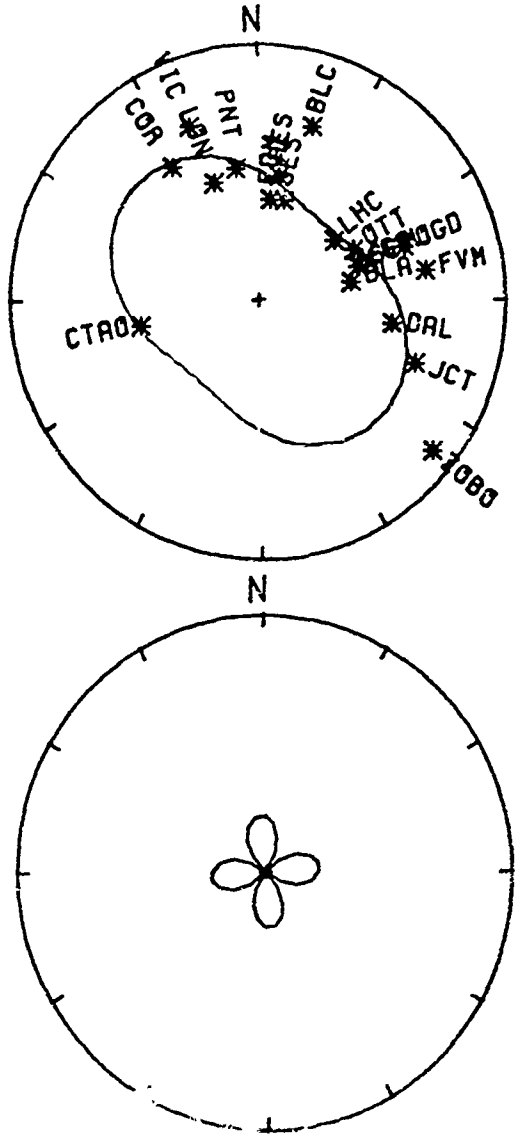

FIGURE 24. Observed and calculated amplitude radiation patterns for the Rayleigh waves (top) and the Love waves (bottom) for the NTS event, MARSILLY. See caption, Figure 12.

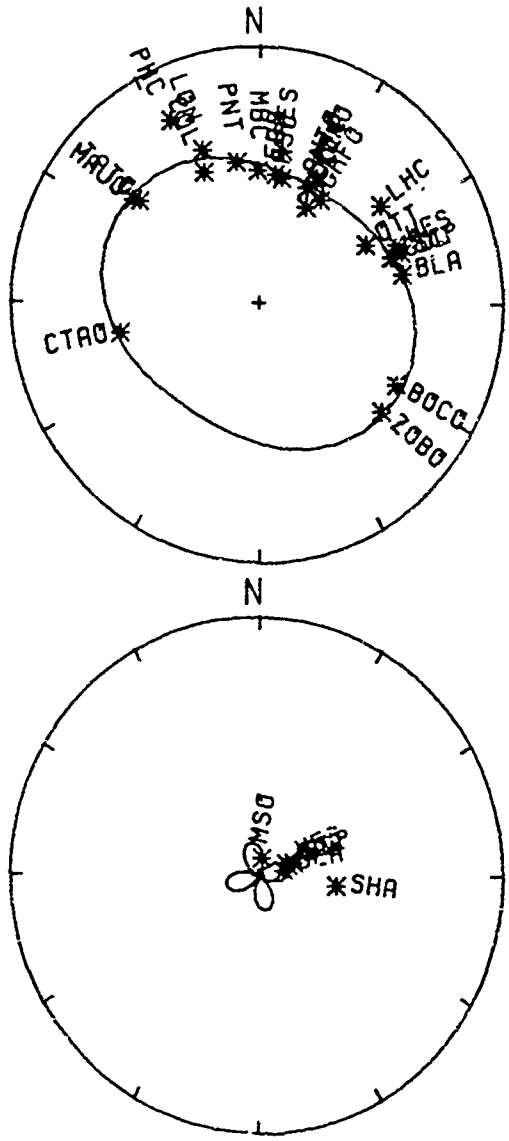

AZIMUTH VS. AVG. SPECTRAL AMPLITUDE
Maximum amplitude= 1.71x 10^{-5} M-s

FIGURE 25. Observed and calculated amplitude radiation patterns for the Rayleigh waves (top) and the Love waves (bottom) for the NTS event, PEPATO. See caption, Figure 12.

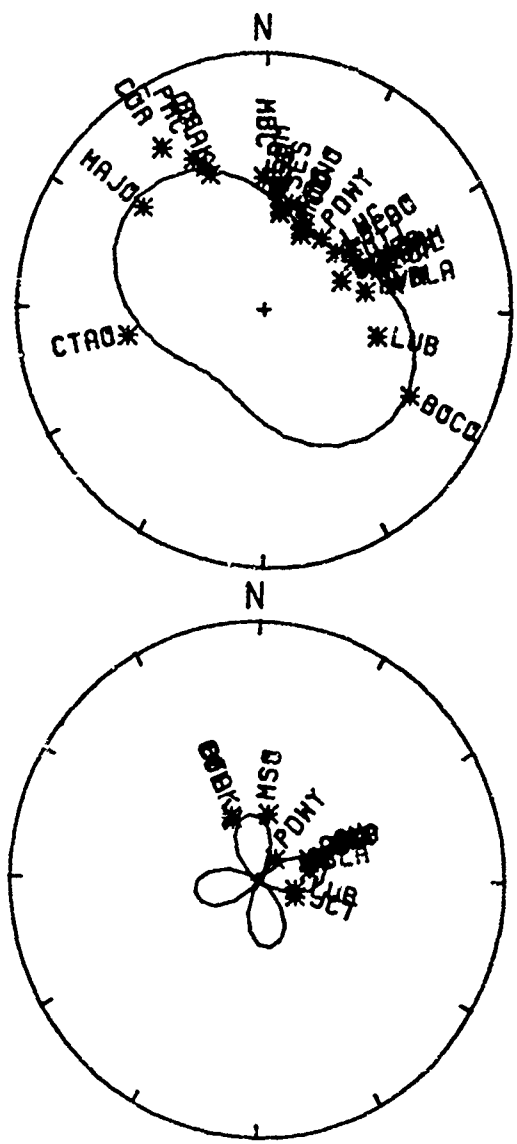

FIGURE 26. Observed and calculated amplitude radiation patterns for the Rayleigh waves (top) and the Love waves (bottom) for the NTS event, HEARTS. See caption, Figure 12.

domain wave-forms vary much more at NTS, both between Pahute Mesa and Yucca Flats and within each subregion. This qualitative observation may be a result of the higher frequencies in the observations due to instrumentation. Some events scatter more than others, as for example the event Marsilly, Figure 24. This event has anomalously low 20 s surface wave amplitudes, by almost a factor of 2, relative to its m_b suggesting much lower coupling at the long periods.

The NTS results are given in Tables 4 and 5. For the NTS events, M_l is determined by assuming a strike-slip fault mechanism. This is in agreement with conclusions reached by previous investigators (e.g., Aki and Tsai, 1971; Toksoz and Kehrer, 1972; Wallace et al., 1985). We can examine the range of feasible fault mechanisms by observing how (0.9 log M_l - m_c) varies with F_{SS}, the F-value derived by assuming a strike slip mechanism. The m_b's forming the NTS events were provided by J. Murphy (personal communication). Figures 27 and 28 show (0.9 log M_l - m_b) vs. F_{SS} for three assumed fault mechanisms for the tectonic release: strike-slip faulting (dip 90, slip 90), oblique thrust faulting (45 30), and oblique normal faulting (45, -30). There is considerable scatter in the correlation between log M_l and m_b, and it is difficult to evaluate the significance of any trend. We simply conclude from these figures that strike slip faulting explains the data as well as any mechanism. The high values of log M_l relative to m_b at Pahute Mesa suggests that some normal component may be present.

The overall correlation between m_b and M_l, assuming a strike-slip mechanism, is shown in Figure 29. As at Shagan River, there appears to be some regional differences in the correlation based on subregion at NTS, although log M_l still scatters over a range of 0.4 at both Yucca Flats and Pahute Mesa. We attribute this to either inhomogeneities in the relative coupling at NTS or variations in the tectonic release mechanism Either alternative cannot be explored further within the period range we are using; analysis at higher frequencies will be necessary.

TABLE 4

PAHUTE MESA

	M_l	Log M_l	F	M_{DC}	STRIKE	m_b
SCOTCH	28.8	1.46	0.40	11.4	91	5.58
STILTON	18.2	1.26	0.26	4.8	95	5.80
STINGER	14.8	1.17	0.35	5.1	91	5.66
SLED	15.9	1.20	0.27	4.2	74	5.87
PURSE	23.2	1.37	0.28	6.4	68	5.77
ALMENDRO	55.8	1 75	0.38	21.0	79	6.17
TYBO	39.9	1.60	0.21	8.3	69	6.01
MAST	49.0	1.69	0.38	18.6	90	6.04
CHESHIRE	44.9	1.65	0.50	24.3	80	5.86
ESTUARY	58.5	1.77	0.35	20.2	79	5.92
POOL	31.7	1.50	0.45	14.2	82	6.01
BACKBEACH	9.4	0.98	0.23	2.2	92	5.49
PANIR	8.3	0.92	0.26	2.2	52	5.65
FARM	8.7	0.94	0.42	3.7	87	5.57
PEPATO	13.3	1.13	0.08	1.1	78	5.58
SHEEPSHEAD	9.6	0.98	0.13	1.3	84	
KASH	13.4	1.13	0.17	2.3	78	5.71
TAFI	12.6	1.10	0.15	2.0	71	

Units of M_l are 10^{15} N-m.

m_b's from Murphy (personal communication)

TABLE 5

YUCCA FLATS

	M_l	Log M_l	F	M_{DC}	STRIKE	m_b
CORDUROY	12.7	1.11	0.39	4.9	82	5.53
DUMONT	12.3	1.09	0.40	5.0	85	5.68
COMMODORE	22.3	1.35	0.28	6.1	94	5.81
ZAZA	19.5	1.29	0.25	4.9	99	5.75
LANPHER	7.0	0.85	0.15	1.0	104	5.66
NOGGIN	10.9	1.04	0.36	3.9	75	5.77
CALABASH	6.8	0.83	0.40	2.8	91	5.61
FLASK	3.6	0.55	0.07	0.23	93	
TIJERAS	10.2	1.01	0.05	0.50	56	5.5
CARPETBAG	13.4	1.13	0.27	3.6	98	5.82
OSCURO	11.6	1.07	0.10	1.1	84	5.67
STARWORT	4.17	0.62	0.07	0.26	61	5.47
ESCABOSA	15.0	1.18	0.18	2.6	69	5.66
PORTMANTEAU	9.3	0.97	0.33	3.1	94	5.72
TOPGALLANT	6.6	0.82	0.25	1.7	86	5.70
MIZZEN	11.6	1.06	0.03	0.33	56	5.63
CHIBERTA	13.9	1.14	0.10	1.5	67	5.74
ESROM	11.1	1.05	0.45	4.9	79	5.67
KEELSON	9.0	0.96	0.26	2.3	78	5.65
STRAIT	16.1	1.21	0.20	3.3	87	5.84
MARSILLY	5.3	0.72	0.15	0.80	85	5.68
SCANTLING	11.1	1.05	0.07	0.82	88	5.61
LOWBALL	6.7	0.82	0.11	0.73	66	5.60
SANDREEF	17.7	1.25	0.32	5.5	83	5.81
FARALLONES	10.9	1.04	0.15	1.7	93	5.77
ICEBERG	10.6	1.02	0.08	0.77	70	5.65
QUINELLA	6.8	0.83	0.10	0.67	79	5.60
RUMMY	14.1	1.15	0.27	3.8	73	
HEARTS	14.3	1.16	0.19	2.8	80	5.84

Units of M_l are 10^{15} N-m.

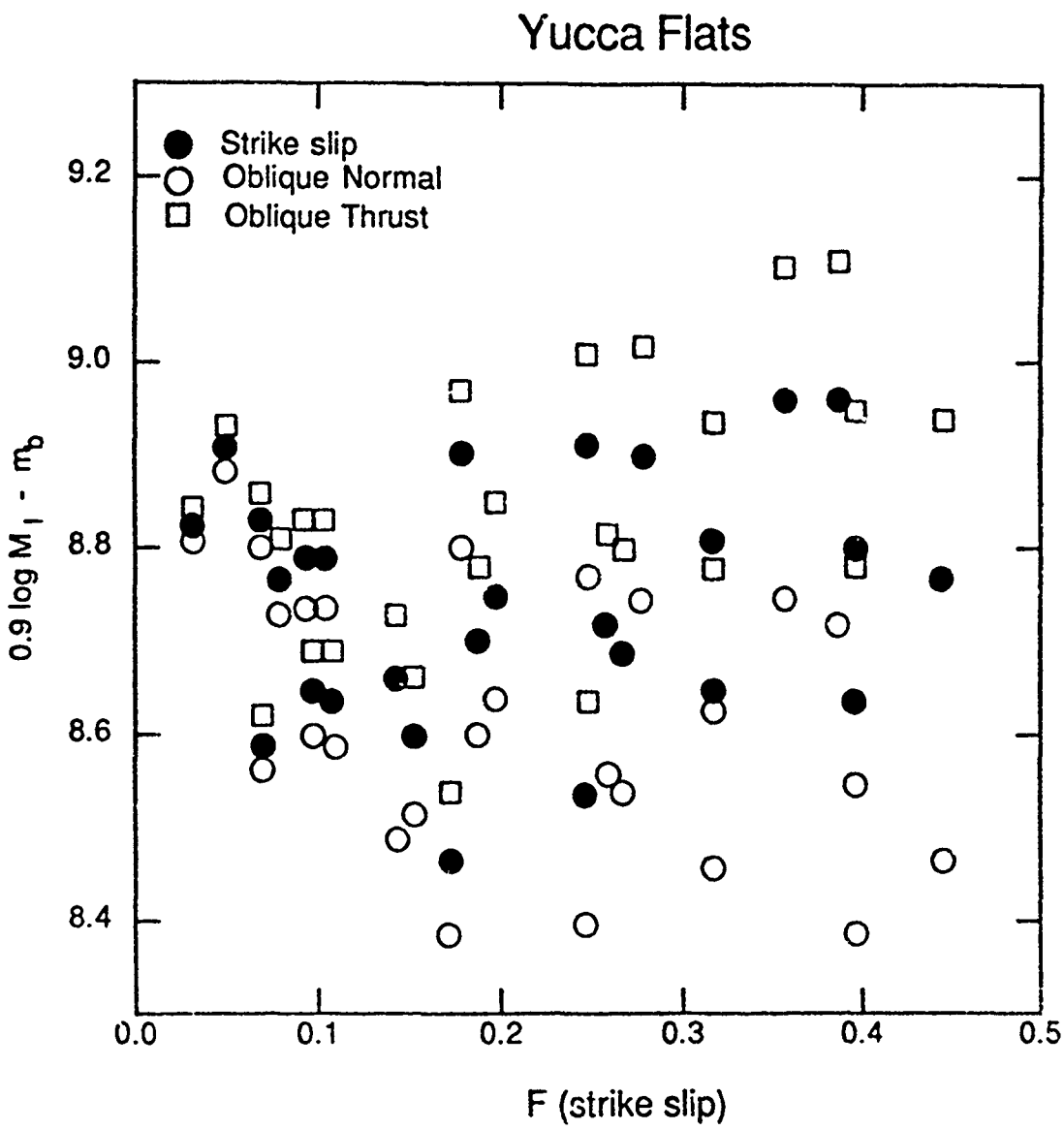

FIGURE 27. The variation of log M_l - m_b relations with F at Yucca Flats for three possible mechanisms of tectonic release: strike slip faulting (dip = 90, ship = 0) oblique normal faulting (dip = 45, slip = -30^o) and oblique thrust faulting (dip = 45, slip = 30^o). For each event the same F is used; F is calculated using the strike slip tectonic release mechanism.

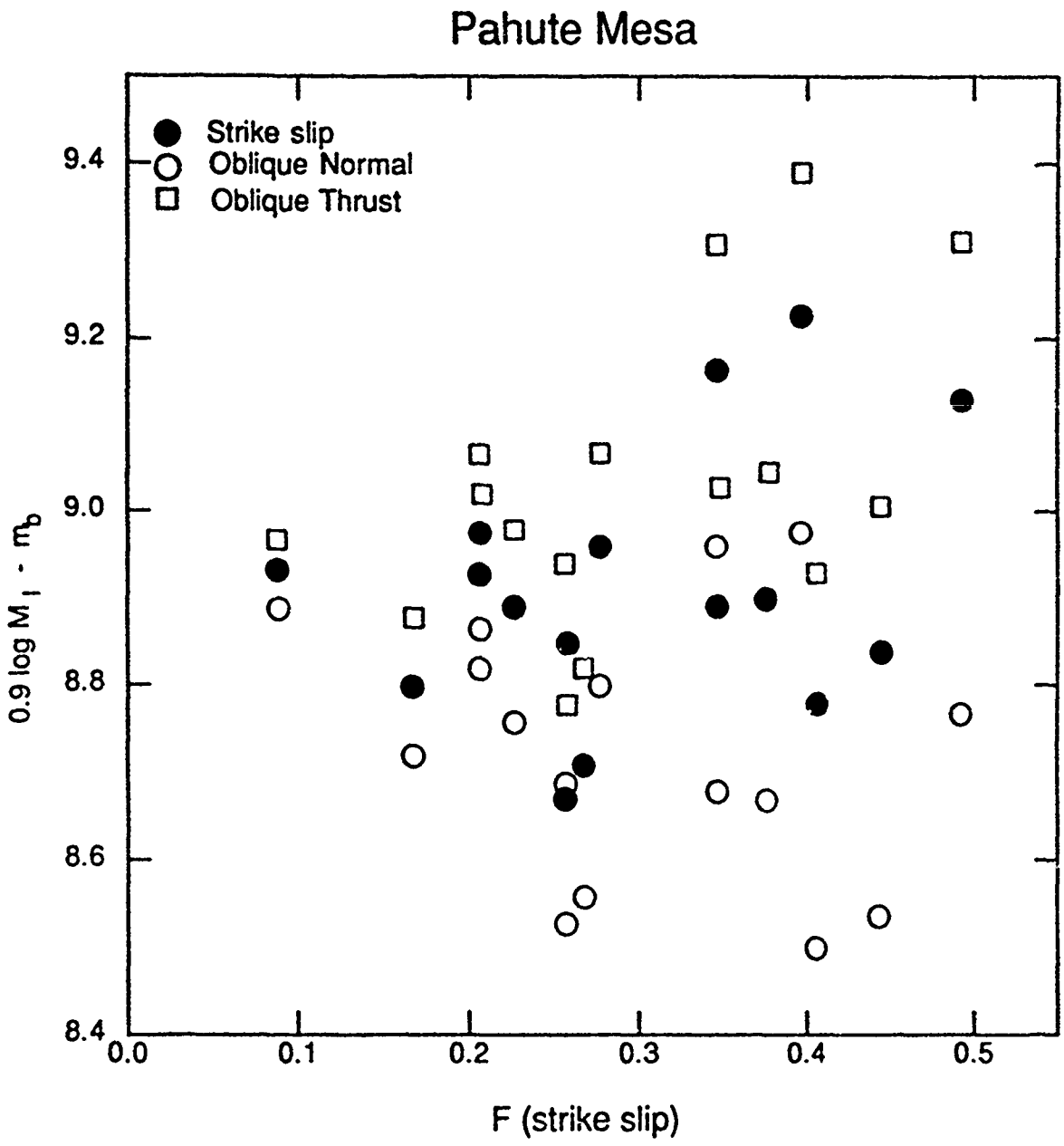

FIGURE 28. The variation in log $M_l - m_b$ relations with F' at Pahute Mesa for three possible mechanisms of tectonic release. See caption, Figure 27.

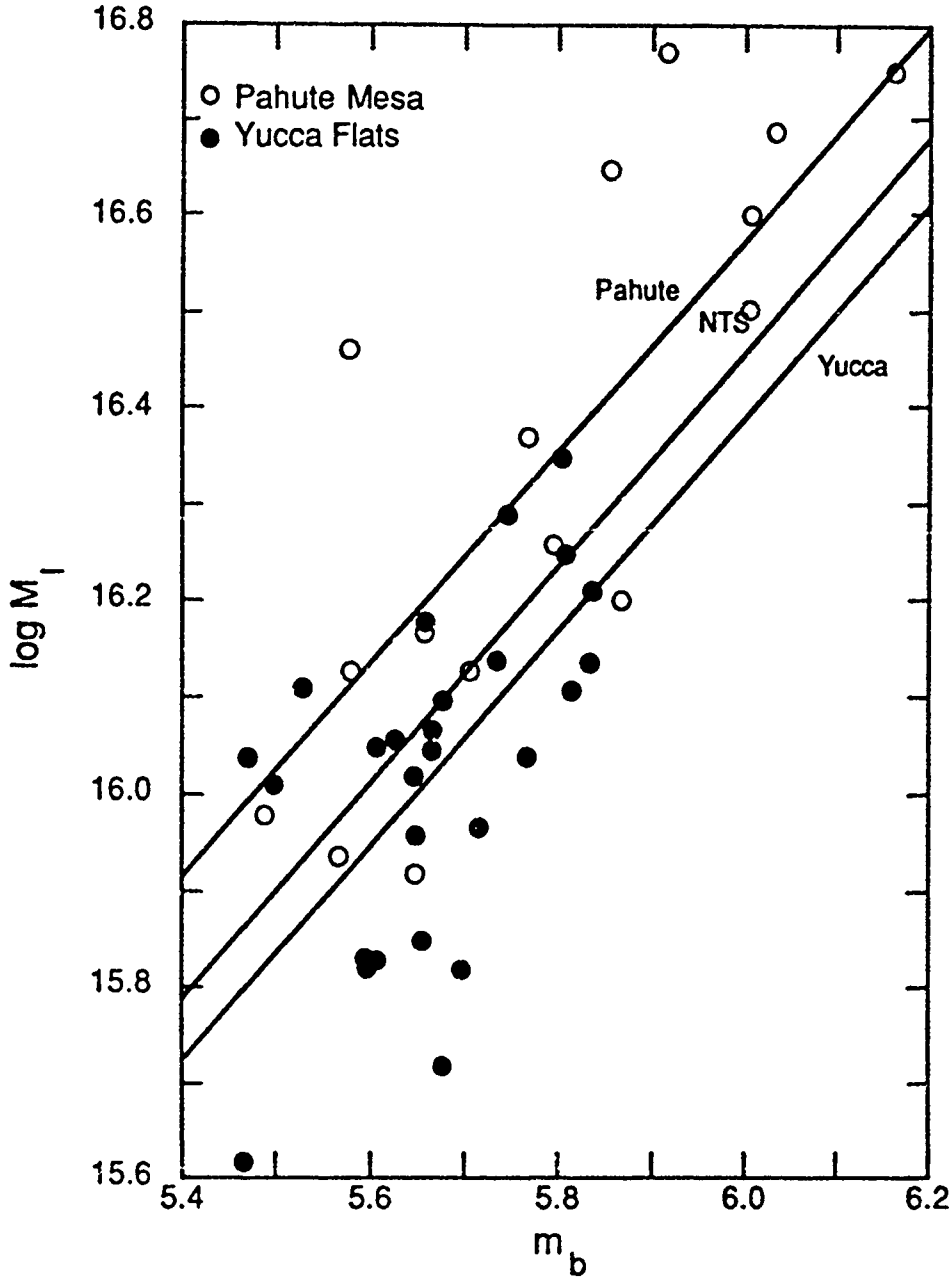

FIGURE 29. Log M_l vs m_b at NTS.

V. DISCUSSION

Several authors (Evernden and Filson, 1971; Marshall and Basham, 1972, Sykes and Cifuentes, 1984; Sykes and Wiggins, 1986) have noted that M_S correlates well with yield independent of test sites and have used M_S to calibrate m_b - yield relations for several regions. Our results, in terms of log M_I, can be used in place of M_S to compare m_b vs. M_I relations between the U.S. and Soviet test sites. The use of the isotropic moments determined in our analysis should have several advantages over previous calibration studies using M_S. The effects of propagation are removed from the observed spectral data using dispersion and attenuation corrections derived for each source to receiver path from direct observation of surface-wave propagation properties. Differences in source excitation are accounted for using the best available estimates of source structure. The excitation of Love and Rayleigh waves are related through a specific model using the radiation patterns to estimate the nonisotropic effects, rather than using an average Love to Rayleigh wave amplitude ratio that is very dependent on station coverage and that does not account for changes in the orientation of the tectonic release. The weakness in these results, as in any source amplitude estimate at long periods, is that the nonisotropic and explosion components for each event cannot be unambiguously resolved. These results, in terms of S_0, S_1 and S_2, represent the most information available at 20 s periods, while the log M_I values rely on interpretation.

If we compare the log M_I versus m_b correlation, shown in Figure 21 with a similar correlation of M_S versus m_b (say, for instance, that of Sykes and Cifuentes, 1984) we find that, overall, there is little improvement in the scatter. Although disappointing, this is not surprising. Two-thirds of these events have an F-value between 0.25 and 0.4 where the typical M_S correction due to tectonic release is between 0.2 and 0.4. With a careful method of simultaneously estimating station corrections and M_S, the effects of the average radiation pattern would be absorbed into the station corrections. The

correlation between m_b and M_S should be similar to the correlation between m_b and log M_l for these events. The scatter in this subset of events is as large as the scatter in the entire population and, therefore, correcting for tectonic release will not dramatically improve the correlation between long-period and short-period measures of explosion strength. The scatter between log M_l and m_b, (or M_S and m_b) cannot be resolved with the tectonic release models presented here.

Although our results do not increase the precision of yield estimates they do provide a more accurate and realistic picture of the source processes at long periods. We have eliminated many of the uncertainties arising from oversimplified attempts to remove propagation effects and we can now begin to attribute anomalous m_b - log M_l behavior to real variations in the source spectra. For example two closely located events in the southwest part of Shagan River, 23 December 1979 and 27 December 1981, show anomalously low amplitude surface waves, relative to their m_b's. Since our values of M_l are the maximum possible, their behavior can only be explained by tectonic release if most of the other events at Shagan River show a substantial amount of strike slip component, more than the oblique-slip model considered earlier. These events must represent real variations in the relative coupling between the long and short periods.

The total effect of the tectonic release is illustrated in Figure 30 by a comparison of isotropic moments derived in three ways. Two sets of results, those that include tectonic release with thrust and oblique-slip faulting, are different interpretations of the same inversion results. The third set of results was derived by inverting observations from those events with F-values less than 0.4 for station corrections and source parameters while constraining each event to be isotropic. This last population should be directly comparable to a conventional M_S determination. For the typical event (median F-value of 0.33), tectonic release reduces the overall amplitude of the Rayleigh waves, as measured by M_S, by 0.3 assuming a thrust mechanism, and 0.2, assuming an oblique-slip mechanism.

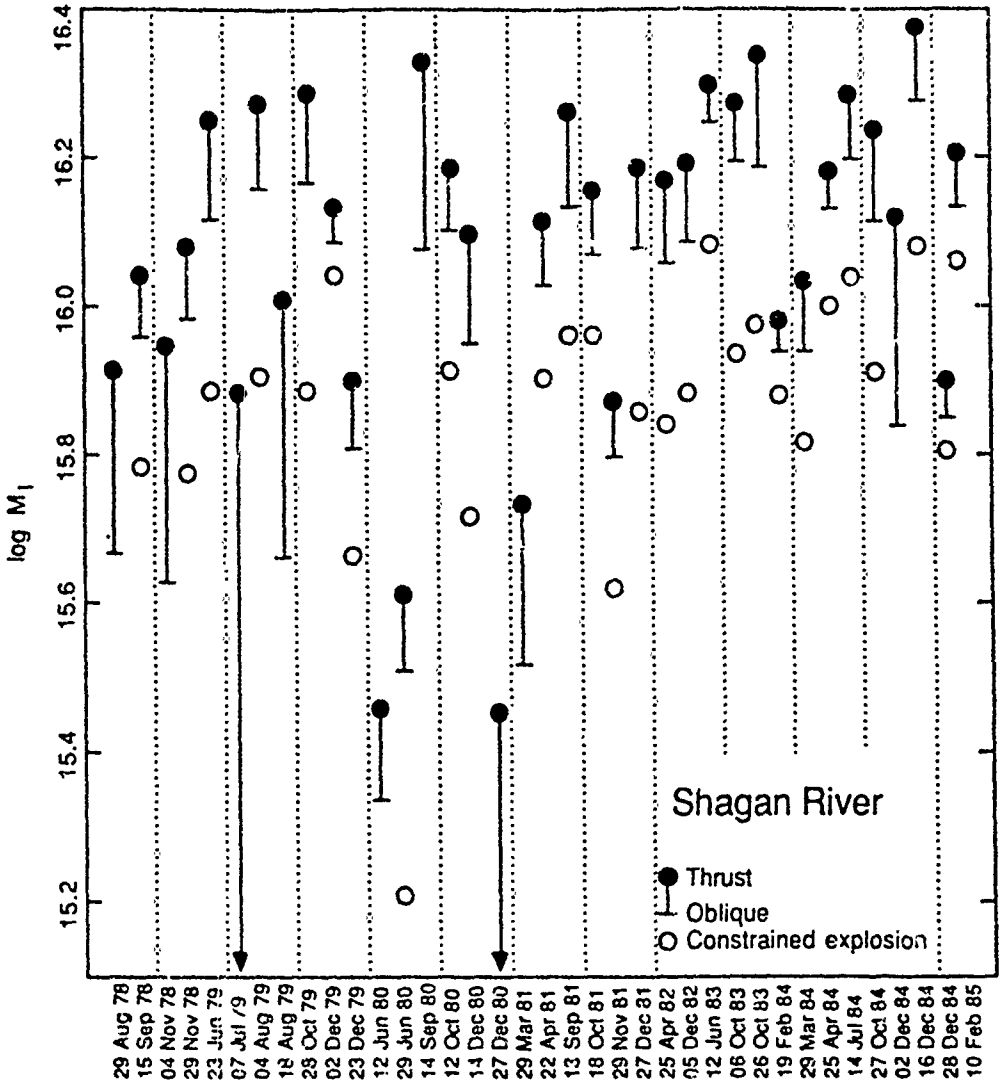

FIGURE 30. Comparison of log M_l for all events at Shagan River.

At NTS, the assumption that strike-slip faulting as the model for the tectonic release suggests that log M_l and M_S will represent the explosion size equally well for the events studied here if the azimuthal coverage is adequate. However, the three parameter source model is better able to account for well-observed, systematic variations in amplitudes due to tectonic release. Figures 31 and 32 compare log M_l derived from inverting Equation 17 for source parameters with and without tectonic release. The two measurements are very similar, which indicates that M_S and log M_l should correlate with yield at NTS to the same precision.

A direct comparison of the largest events at each test site reveals that, assuming a thrust-fault tectonic release mechanism, log M_l of the largest Shagan River explosions (~16.3) is about 0.1 higher than the largest Yucca Flats events and about 0.15 higher than the largest Pahute Mesa events. With the oblique-slip mechanism the largest events at Shagan River are comparable to the largest NTS events.

The m_b vs. M_l relations from NTS are summarized in Figure 29. For a given M_l, m_b from an event at Yucca Flats is 0.2 magnitude units lower than one at Pahute Mesa. This feature may be explained by changes in the P-wave velocity in the vicinity of the shot point. If Poissons ratio is the same for the two areas, than Stevens and Day (1985) show that

$$D\ (m_b - \log M_l) = D \log (\rho\alpha^3)\ 1/2 \qquad (23)$$

If d goes from 2.5 at Yucca to 3.5 at Pahute the observed differences can be explained. This is a result of changes in the body-wave excitation and so we might expect m_b - yield relations to show a similar discrepancy.

Direct comparison of the overall NTS and Shagan River m_b-M_l relations can give an estimate of the difference in m_b between similar sized events at the two test sites. Table 6 compares the m_b - M_l relations for three regionalizations at NTS and at Shagan River. For a given

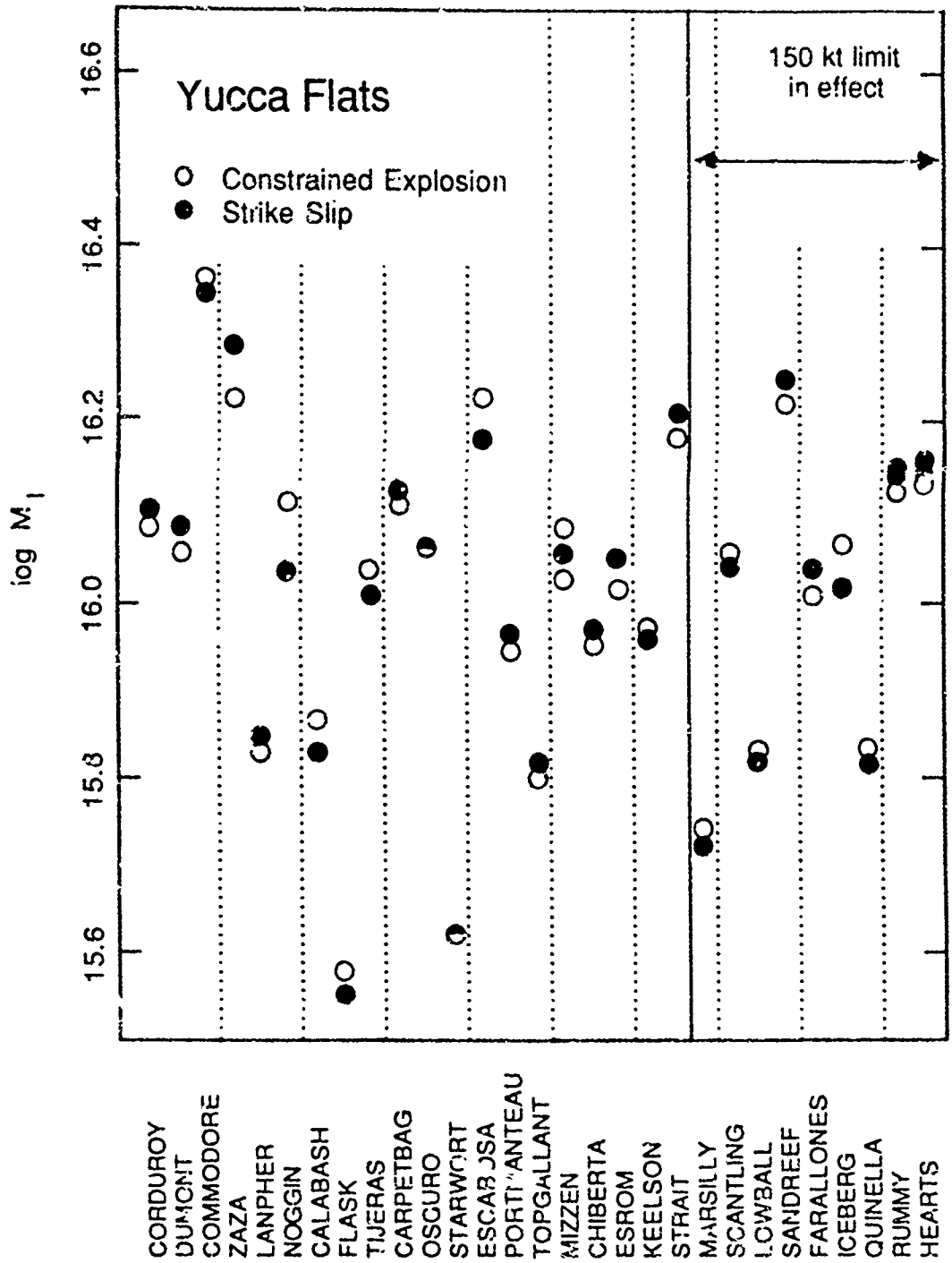

FIGURE 31. Comparison of log M_l for the Yucca Flats events.

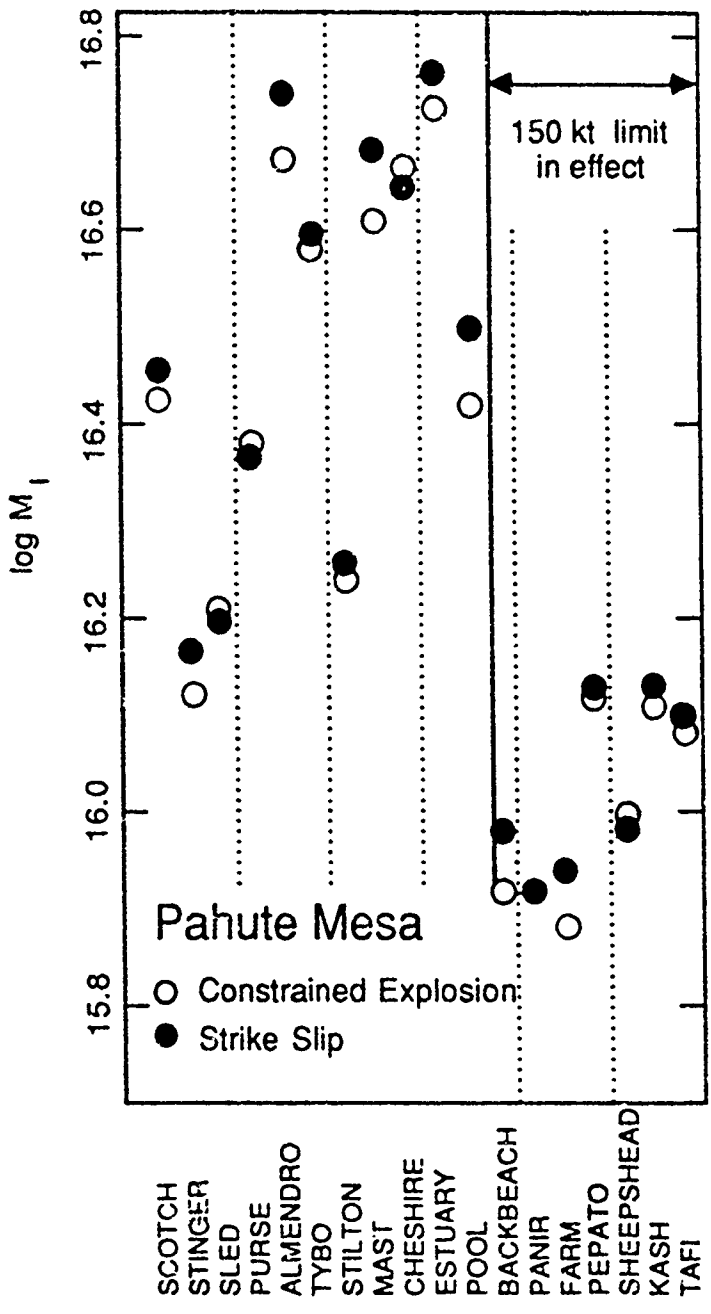

FIGURE 32. Comparison of log M_l for the Pahute Mesa events.

TABLE 6

m_b - log M_l RELATIONS AT NTS AND SHAGAN RIVER

SHAGAN RIVER

13 Southwest events with error in log M_l < 0.06 (13)
and consistent m_b (from Marshall et al. 1984)
$m_b = 0.9 \log M_l - 8.43$ ($\sigma = 0.11$)

27 All events with error in log M_l < 0.06 (27)
$m_b = 0.9 \log M_l - 8.49$ ($\sigma = 0.14$)

37 events
$m_b = 0.9 \log M_l - 8.48$ ($\sigma = 0.16$)

NTS

16 Pahute Mesa events:
$m_b = 0.9 \log M_l - 8.92$ ($\sigma = 0.15$)

27 Yucca Flats events:
$m_b = 0.9 \log M_l - 8.75$ ($\sigma = 0.13$)

43 NTS events:
$m_b = 0.9 \log M_l - 8.81$ ($\sigma = 0.16$)

M_l, an event at Shagan River has an m_b that is about 0.3 higher than an event at NTS. This m_b bias is consistent with previous estimates, including those derived from Sykes and Cifuentes, 1984, Marshall et al., 1979 and Der et al., 1985.

VI. SUMMARY AND CONCLUSIONS

The long-period (~20 s) Rayleigh and Love waves for 37 events at Shagan River and 47 events at NTS are inverted for source parameters using the best available information on propagation for each source-receiver path and on excitation for each source region. At these periods, a three parameter source model is sufficient to describe the Rayleigh and Love wave amplitude and phase radiation patterns. However, the scatter in the source amplitudes dominates the radiation patterns of the surface waves, and additional station correction factors are necessary. These corrections are derived by simultaneously inverting many events from each test site for both the source parameters and station corrections. The inclusion of both Love and Rayleigh waves for events with a wide range of relative Love to Rayleigh wave excitation reduces possible bias in the station corrections. This feature is important because no events at either test site are free from tectonic release effects.

The three source parameters do not constrain the size of the explosion source and further interpretation is necessary. In this study, m_b is assumed to reflect the explosion size. For an assumed tectonic release mechanism, we assume that there should be no correlation betwsen (0.9 log M_l - m_b) and the amount of tectonic release present. At Shagan River, the tectonic release mechanism must include a substantial thrust-faulting component; at NTS, a strike slip fault model for the tectonic release is appropriate.

With the thrust fault model, the Rayleigh waves from the typical (median) event ($F = M_l/M_{DC} = 0.33$) at Shagan River are reduced in amplitude by the effects of tectonic release by 0.3 as measured by M_S (or log M_l). The overall correlation between log M_l and m_b at Shagan River is not expected to be any better than M_S and m_b. At NTS, log M_l, derived assuming tectonic release, is very similar to log M_l derived assuming no tectonic release. We do not anticipate any difference in the overall precision of yield estimates using log M_l or M_S at NTS.

The explosion moments of the largest events at Shagan River are slightly higher (δ log M_l = 0.1) than the largest events analyzed from NTS. m_b at Pahute Mesa is 0.2 higher than an event at Yucca Flats with a similar M_l. For a given M_l, an event at Shagan River is expected to have an m_b that is 0.32 higher than an event at NTS.

VII. REFERENCES

Aki, K., P. Reasonberg, T. De Fazio and Y.B. Tsai, 1969, Near-field and far-field seismic evidences for triggering of an earthquake by the Benham explosion, Bull. Seism. Soc. Am., 59, 2197-2207

Aki, K. and T. Yi-Ben, 1972, Mechanism of Love-Wave excitation by explosive sources, J. Geophys. Res., 77, 1452-1475

Anderson, D.L. and R.S. Hart, 1976, An earth model based on free oscillations and body waves, J. Geophys. Res., 81, 1461-1475

Anderson, D.L. and R.S. Hart, 1978, Q of the earth, J. Geophys. Res., 83, 5869 5882

Archambeau, C.B., 1972, The theory of stress wave radiation from explosions in prestressed media, Geophys. J. R. Astr. Soc., 29, 329-366

Bache, T.C., T.R. Blake, J.T. Cherry, T.G. Barker, D.G. Lambert, J.M. Savino and N. Runer, 1975, An explanation of the relative amplitudes of the teleseismic body waves generated by explosions in different test areas at NTS, Systems, Science and Software Final Report DNA TR No. 3958F (SSS-R-76-2746)

Bache, T.C. and D.G. Lambert, 1976, The seismological evidence for the triggering of block motion by large explosions, Systems Science and Software Topical Report SSS-R-77-3118, submitted to Defense Nuclear Agency, December

Bache, T.C., W.L. Rodi and D.G. Harkrider, 1978, Crustal structures inferred from Rayleigh wave signatures of NTS explosions, Bull. Seism. Soc. Am., 68, 1399-1413

Bache, T.C., P.D. Marshall and L.B. Bache, 1985, Q for teleseismic P waves from central Asia, J. Geophys. Res., 90, 3575-3588

Burger, R.W., T. Lay, C.G. Arveson and L.J. Burdick, 1985, Estimating seismic yield, pP parameters and tectonic release characteristics at the Novaya Zemlya test site, Woodward-Clyde Consultants Final Technical Report WCCP-R-85-03, Contract No. AFOSR/NP F49620-83-C-0028 P-4.

Bucknam, R.C., 1969, Geologic effects of the Benham underground nuclear explosion, Bull. Seism. Soc. Am., 59, 2209-2220

Der, Z.A., T.W. McElfresh, R. Wagner and J. Burnetti, 1985, Spectral characteristics of P-waves from nuclear explosions and yield estimation, Bull. Seism. Soc. Am., 75, 379-390

Evernden, J.F. and J. Filson, 1971, Regional dependence of surface wave versus body wave magnitudes, J. Geophys. Res., 76, 3303-3308

Goforth, T., B. Rafipour and E. Herrin, 1982, Anomalous Rayleigh waves from nuclear explosions at the USSR Shagan Riger test site, in: Herrin, E. and Goforth, T., AFOSR Semiannual Technical Report, Geophysical Laboratory, Southern Methodist University

Hamilton, R.M. and J.H. Healy, 1969, Aftershocks of the Benham nuclear explosion, Bull. Seism. Soc. Am., 59, 2271-2282

Helle, H.B. and E. Rygg, 1984, Determination of tectonic release from surface waves generated by nuclear explosions in Eastern Kazakhstan, Bull. Seism. Soc. Am., 74, 1883-1898

Herrin, E. and T. Goforth, 1977, Phase-matched filters: application to the study of Rayleigh waves, Bull. Seism. Soc. Am., 67, 1259-1275.

Kanamori, H. and G.S. Stewart, 1976, Mode of the strain release along the Gibbs Fracture Zone, Mid-Atlantic Ridge, Phys. Earth Planet. Int. 11, 312-332.

Kanamori, H. and J.W. Given, 1981, Use of long-period surface waves for rapid determination of earthquake-source parameters, Phys. Earth Planet Int., 27, 8-31

Lay, T., T.C. Wallace and D.V. Helmberger, 1984, The effects of tectonic release on short period P-waves from NTS explosions, Bull. Seism. Soc. Am., 74, 819-842

North, R.G. and T.J. Fitch, 1981, Surface wave generation by underground nuclear explosions, Semiannual Technical Summary, March 31, No. ESD-TR-81-84 (Lincoln Laboratory, Mass. Inst. of Tech., Cambridge, Mass.), 47-55 ADA109/84

Marshall, P.D. and P.W. Basham, 1972, Discrimination between earthquakes and underground explosions employing an improved M_S scale, Geophys. J.R. Astr. Soc., 28, 431-458

Marshall, P.D., D.L. Springer and H.C. Rodean, 1979, Magnitude corrections for attenuation in the upper mantle, Geophys. J.R. Astr. Soc., 57, 609-638

Marshall, P.D., T.C. Bache and R.C. Lilwall, 1984, Body wave magnitudes and locations of Soviet underground explosions at the Semipalatinsk test site, Atomic Weapons Res. Establishment Report 0 16/84

Press, F. and C. Archambeau, 1962, Release of tectonic strain by underground nuclear explosions, J. Geophys. Res., 667, 337-343

Rygg, E., 1979, Anomalous surface waves from underground explosions, Bull. Seism. Soc. Am., 69, 1995-2000

Stevens, J.L., W.L. Rodi, J. Wang, B. Shkoller, E.J. Halda, B.F. Mason and J.B. Minster, 1982, Surface wave analysis package and Shagan River to SRO station path corrections, S-Cubed Topical Report VSC-TR-82-21

Stevens, J.L., 1986, Estimation of scalar moments from explosion-generated surface waves, Bull. Seism. Soc. Am., 76, 123-152

Stevens, J.L. and S.M. Day, 1985, The physical basis of m_b:M_S and variable frequency magnitude methods of earthquake/ explosion discrimination, J. Geophys. Res., 90, 3009-3020

Sykes, L.R. and I.L. Cifuentes, 1984, Yields of Soviet underground nuclear explosions from seismic surface waves: compliance with the Threshold Test Ban Treaty, Proc. Natl. Acad. Sci. USA, 81, 1922-1925

Sykes, L.R. and G.C. Wiggins, 1985, Yields of Soviet underground nuclear explosions, Novaya Zemlya, 1964-1976 from seismic body and surface waves, Proc. Natl. Ac. Sci. USA, (submitted) 1985

Toksoz, M.N., A. Ben-Menahem and D.G. Harkrider, 1965, Determination of source parameters of explosions and earthquakes by amplitude equalization of seismic surface waves; release of tectonic strain by underground nuclear explosions and mechanisms of earthquakes, J. Geophys. Res., 70, 907-922

Toksoz, M.N. and H.H. Kehrer, 1972, Tectonic strain release by underground nuclear explosions and its effect on seismic discrimination, Geophys. J. R. Astr. Soc., 31, 141-161

Wallace, T.C., D.V. Helmberger and G.R. Engen, 1983, Evidence of tectonic release from underground nuclear explosions in long-period P waves, Bull. Seism. Soc. Am., 73, 593-613

Wallace, T.C., D.V. Helmberger and G.R. Engen, 1985, Evidence of tectonic release from underground nuclear explosions in long period S waves, Bull. Seis. Soc. Am., 75, 157-174